Available online at www.sciencedirect.com

ScienceDirect

Advances in Mathematics 219 (2008) 894–931

ADVANCES IN Mathematics

www.elsevier.com/locate/aim

Asymptotics of Plancherel measures for the infinite-dimensional unitary group

Alexei Borodin *, Jeffrey Kuan

California Institute of Technology, Department of Mathematics 253-37, Pasadena, CA, United States

Received 8 January 2008; accepted 9 June 2008

Available online 18 July 2008

Communicated by the Managing Editors of AIM

Abstract

We study a two-dimensional family of probability measures on infinite Gelfand–Tsetlin schemes induced by a distinguished family of extreme characters of the infinite-dimensional unitary group. These measures are unitary group analogs of the well-known Plancherel measures for symmetric groups.

We show that any measure from our family defines a determinantal point process on $\mathbb{Z}_+ \times \mathbb{Z}$, and we prove that in appropriate scaling limits, such processes converge to two different extensions of the discrete sine process as well as to the extended Airy and Pearcey processes.

Keywords: Plancherel measures; Infinite-dimensional unitary group; Determinantal point processes

Contents

* Corresponding author.
E-mail address: borodin@caltech.edu (A. Borodin).

0001-8708/$ – see front matter
doi:10.1016/j.aim.2008.06.012

1. Introduction

Let $S(n)$ be the symmetric group of degree n. Denote by $\mathbb{Y}_n$ the set of partitions of n or, equivalently, the set of Young diagrams with n boxes. It is well known that complex irreducible representations of $S(n)$ are parameterized by elements of $\mathbb{Y}_n$; we denote by $\dim\lambda$ the dimension of the irreducible representation corresponding to λ. The probability distribution

$$\mathrm{Prob}\{\lambda\} = \frac{\dim^2\lambda}{n!}, \quad \lambda \in \mathbb{Y}_n,$$

on $\mathbb{Y}_n$ is called the *Plancherel measure* for $S(n)$. The Plancherel weight of $\lambda \in \mathbb{Y}_n$ is the relative dimension of the isotypic component of the regular representation of $S(n)$, which transforms according to the irreducible representation corresponding to λ. Hence, one has the following equality of functions on $S(n)$:

$$\delta_e = \sum_{\lambda\in\mathbb{Y}_n} \frac{\dim^2\lambda}{n!}\frac{\chi^\lambda}{\dim\lambda},$$

where δ_e is the delta-function at the unity, and χ^λ is the irreducible character corresponding to λ.

Let $S(\infty) = \bigcup_{n\geqslant 1} S(n)$ be the group of finite permutations of a countable set known as the *infinite symmetric group*, see e.g. [21]. The group $S(\infty)$ has a rich theory of characters (positive-definite central functions on the group). For any character χ of $S(\infty)$ normalized by $\chi(e) = 1$, its restriction to the subgroup $S(n)$ of permutations of first n symbols can be written as

$$\chi = \sum_{\lambda\in\mathbb{Y}_n} \hat{\chi}_n(\lambda)\chi^\lambda/\dim\lambda.$$

The coefficients $\hat{\chi}_n(\lambda)$ form a probability measure on $\mathbb{Y}_n$; they are a kind of Fourier transform of χ.

There exists only one character χ of $S(\infty)$ for which the rows and columns of the Young diagrams distributed according to $\hat{\chi}_n$ grow sublinearly in n as $n \to \infty$. This character is the delta-function at the unity of $S(\infty)$, the corresponding representation is the (bi)regular representation of $S(\infty)$ in $\ell^2(S(\infty))$, and $\hat{\chi}_n$ is the Plancherel measure on $\mathbb{Y}_n$ introduced above.

An analogous construction for the *infinite-dimensional unitary group* $U(\infty) = \bigcup_{N\geqslant 1} U(N)$ yields a two-dimensional family of characters of $U(\infty)$. Equip $U(\infty)$ with the direct limit topology. Although the notion of regular representation for $U(\infty)$ is meaningless, by comparing the lists of the *extreme* (i.e., indecomposable) characters of $S(\infty)$ and $U(\infty)$ one sees that the analog of δ_e on $S(\infty)$ is the family of characters

$$\chi^{\gamma^+,\gamma^-}(U) = \exp\bigl(\operatorname{Tr}\bigl(\gamma^+(U-1)+\gamma^-\bigl(U^{-1}-1\bigr)\bigr)\bigr), \quad U \in U(\infty),$$

where $\gamma^\pm \geqslant 0$ are the parameters of the family. We will provide details in Section 3, and for now let us just say that on the level of Fourier transform, the set $\mathbb{Y}_n$ is replaced by the set of N-tuples of integers $\lambda_1 \geqslant \cdots \geqslant \lambda_N$ which we call *signatures* or *highest weights* of length N (they parameterize irreducible representations of the unitary group $U(N)$), and the corresponding probability distributions have the form

$$P_N^{\gamma^+,\gamma^-}(\lambda_1,\ldots,\lambda_N) = \text{const}\cdot\det\bigl[f_i^{(\gamma^+,\gamma^-)}(\lambda_j-j)\bigr]_{i,j=1}^N \dim_{U(N)}(\lambda),$$

$$f_k^{(\gamma^+,\gamma^-)}(x) = \frac{1}{2\pi i}\oint_{|z|=1} \frac{e^{\gamma^+ z+\gamma^- z^{-1}}\,dz}{z^{x+k+1}}, \quad k=1,2,\ldots,$$

where $\dim_{U(N)}(\lambda)$ is the dimension of the irreducible representation of $U(N)$ with highest weight λ. We call the measures $P_N^{\gamma^+,\gamma^-}$ *the Plancherel measures for the infinite-dimensional unitary group*, and the present paper is devoted to the study of these measures.

One source of interest to the Plancherel measures for symmetric groups is the fact that the distribution of the largest part of $\lambda \in \mathbb{Y}_n$ coincides with the distribution of the longest increasing subsequence of uniformly distributed permutation in $S(n)$. This fact can be restated in terms of a random growth model in one space dimension called the polynuclear growth process (PNG). Namely, the distribution of the height function for PNG with the so-called droplet initial condition at any given point in space-time coincides with the distribution of the largest part of $\lambda \in \bigcup_{n\geqslant 0}\mathbb{Y}_n$ distributed according to the *Poissonized* Plancherel measure

$$\text{Prob}\{\lambda\} = e^{-\theta^2}\left(\frac{\theta^{|\lambda|}\dim\lambda}{|\lambda|!}\right)^2, \quad \lambda \in \bigcup_{n\geqslant 0}\mathbb{Y}_n,$$

where $|\lambda|$ is the number of boxes in the Young diagram λ, and $\theta > 0$ is a parameter, see [30]. Note that $|\lambda|$ is Poisson distributed with mean θ^2.

Quite similarly, the largest coordinate of a signature distributed according to the Plancherel measure for $U(\infty)$ describes the height function in another growth model in one space dimension called PushASEP for the so-called step initial condition. This fact can be established by direct comparison of Proposition 3.4 from [6] and Theorem 3.1 below.

The asymptotics of the Plancherel measure for $S(n)$ as $n\to\infty$ has been extensively studied. In the seventies, Logan and Shepp [22] and, independently, Vershik and Kerov [32,34], discovered that Plancherel distributed Young diagrams have a *limit shape*: In a suitable metric, the measure on these Young diagrams scaled by $\sqrt{n}$ converges as $n\to\infty$ to the delta-measure supported on a certain shape. In the late nineties, more refined results were obtained. It was shown that the random point process generated by the rows (or columns) of the Plancherel distributed Young diagrams has two types of scaling limits, in the "bulk" and at the "edge" of the limit shape. In the limit, the former case yields the discrete sine determinantal point process, while the latter case yields the Airy determinantal point process, see [2,3,8,18,24].

The main goal of the present paper is to prove similar asymptotics results on scaling limits of random point processes related to more complex measures $P_N^{\gamma^+,\gamma^-}$ with $N\to\infty$ and $\gamma^\pm$ possibly dependent on N. Note that our results do not imply the existence of the limit shape in

any of the cases we consider, although they strongly suggest that in some cases the limit shape does exist, and they predict what it looks like. For a discussion of the relationship between "local" results on point processes and "global" measure concentration properties see Remark 1.7 of [8], §1 of [11].

Let us describe our results in more detail.

It is convenient to represent a signature $\lambda = \{\lambda_1 \geqslant \cdots \geqslant \lambda_N\}$ as a pair of partitions, one partition λ^+ consists of positive parts of λ while the other one λ^- consists of absolute values of negative parts of λ. When the parameters $\gamma^\pm$ are independent of N, they describe (see Section 2) the asymptotic behavior of $|\lambda^\pm|$, namely $|\lambda^\pm| \sim \gamma^\pm N$, as $N \to \infty$. This asymptotic relation remains true in other situations as well, and it is helpful to keep it in mind when going through the limit transitions below.

Our first result describes what happens when $\gamma^\pm \sim N^{-1}$ as $N \to \infty$. Then one expects that $|\lambda^+|, |\lambda^-|$ remain finite in the limit, and indeed the measures $P_N^{(\gamma^+,\gamma^-)}$ converge to the product of two independent copies of the Poissonized Plancherel measures for the symmetric groups. One copy is supported on the partitions λ^+ consisting of positive parts, while the other measure is supported on the partitions λ^- consisting of negative parts.

The next possibility to consider is when $\gamma^\pm$ are independent of N. The case when $\gamma^- = 0$ was considered by Kerov [20], who proved the existence of the limit shape and showed that the limit shape coincides with that for the Plancherel measures for symmetric groups. We show that when both parameters $\gamma^\pm$ are fixed and nonzero, the random point processes describing $\lambda^\pm$ asymptotically behave as though $\lambda^\pm$ represent two independent copies of the Poissonized Plancherel measures for the symmetric group with Poissonization parameters $\gamma^\pm N \to \infty$.

The most interesting case is when $\gamma^\pm$ grow at the same rate as N. Biane [4] proved that when $\gamma^- = 0$, the corresponding measure has a limit shape that depends on the limiting value of the ratio γ^+/N. We consider the case when both parameters are nonzero and investigate the asymptotic behavior of the random point process that describes our random signatures.

Even though we do not prove the existence of the limit shape, it is convenient to use the hypothetical limit shape inferred from the limit of the density function to describe the results. There are three possibilities: The limit shapes of $\lambda^\pm$ scaled by N do not touch (that happens when $\gamma^\pm/N$ are small), when they barely meet, and when they have already met, see Fig. 4 in the body of the paper. Accordingly, there are three types of local behavior one can expect: The bulk, the edge, where the limit shape becomes tangent to one of the axes, and the point when the edges of the limit shapes for $\lambda^\pm$ meet. We compute the local scaling limits of the correlation functions for the random point process describing our signatures, and obtain the correlation functions of the discrete sine, Airy, and Pearcey determinantal processes in the three cases above, see Theorems 4.6, 4.9, and 4.8.

As a matter of fact, we consider probability measures on a more general object than signatures. Every character of $U(\infty)$ naturally defines a probability measure on Gelfand–Tsetlin schemes (a kind of infinite semistandard Young tableaux), see Section 2 and [9]. The corresponding measures on signatures of length N are certain projections of the measure on Gelfand–Tsetlin schemes. In particular, every character from our two-dimensional Plancherel family yields a measure on Gelfand–Tsetlin schemes, and that is what we study asymptotically. We interpret each scheme as a point configuration in $\mathbb{Z} \times \mathbb{Z}_+$, and compute the scaling limits of correlation functions of the arising two-dimensional random point processes. The results are appropriate (determinantal) time-dependent extensions of the limiting processes mentioned above.

The proofs are based on the techniques of determinantal point processes.

First, we show that for any extreme character of $U(\infty)$, the corresponding random point process on $\mathbb{Z} \times \mathbb{Z}_+$ is determinantal, and we compute the correlation kernel in the form of a double contour integral of a fairly simple integrand. This result (Theorem 3.1) is similar in spirit to the formula for the correlation kernel of the Schur process from [27], but it does not seem to be in direct relationship with it. After that we perform the asymptotic analysis of the contour integrals largely following the ideas of [25,27,28].

2. Description of the model

Let $U(N)$ denote the group of all $N \times N$ unitary matrices. It is a classical result that the irreducible representations of $U(N)$ can be parametrized by nonincreasing sequences $\lambda = (\lambda_1 \geqslant \cdots \geqslant \lambda_N)$ of N integers (see e.g. [36]). Such sequences are called *signatures (or highest weights) of length N*. Thus there is a natural bijection $\lambda \leftrightarrow \chi^\lambda$ between signatures of length N and the conventional irreducible characters of $U(N)$.

For each N, $U(N)$ is naturally embedded in $U(N+1)$ as the subgroup fixing the $(N+1)$th basis vector. Equivalently, each $U \in U(N)$ can be thought of as an $(N+1) \times (N+1)$ matrix by setting $U_{i,N+1} = U_{N+1,j} = 0$ for $1 \leqslant i, j \leqslant N$ and $U_{N+1,N+1} = 1$. The union $\bigcup_{N=1}^{\infty} U(N)$ is denoted $U(\infty)$.

A *character* of $U(\infty)$ is a positive definite function $\chi : U(\infty) \to \mathbb{C}$ which is constant on conjugacy classes and normalized ($\chi(e) = 1$). We further assume that χ is continuous on each $U(N) \subset U(\infty)$. The set of all characters of $U(\infty)$ is convex, and the extreme points of this set are called *extreme characters*.

The extreme characters of $U(\infty)$ can be parametrized as follows: Let $\mathbb{R}^\infty$ denote the product of countably many copies of $\mathbb{R}$. Let Ω be the set of all $(\alpha^+, \alpha^-, \beta^+, \beta^-, \delta^+, \delta^-)$ such that [29, §1]

$$\alpha^\pm = \left(\alpha_1^\pm \geqslant \alpha_2^\pm \geqslant \cdots \geqslant 0\right) \in \mathbb{R}^\infty, \qquad \beta^\pm = \left(\beta_1^\pm \geqslant \beta_2^\pm \geqslant \cdots \geqslant 0\right) \in \mathbb{R}^\infty, \qquad \delta^\pm \in \mathbb{R},$$

$$\sum_{i=1}^{\infty} \left(\alpha_i^\pm + \beta_i^\pm\right) \leqslant \delta^\pm, \qquad \beta_1^+ + \beta_1^- \leqslant 1.$$

Set

$$\gamma^\pm = \delta^\pm - \sum_{i=1}^{\infty} \left(\alpha_i^\pm + \beta_i^\pm\right) \geqslant 0.$$

For any $U \in U(\infty)$ define Spectrum(U) as the finite set of eigenvalues (with multiplicities) of U that not equal to 1. Each $\omega \in \Omega$ defines a function χ^ω on $U(\infty)$ by

$$\chi^\omega(U) = \prod_{u \in \text{Spectrum}(U)} f_0(u),$$

$$f_0(u) = e^{\gamma^+(u-1)+\gamma^-(u^{-1}-1)} \prod_{i=1}^{\infty} \frac{1+\beta_i^+(u-1)}{1-\alpha_i^+(u-1)} \frac{1+\beta_i^-(u^{-1}-1)}{1-\alpha_i^-(u^{-1}-1)}. \tag{1}$$

As ω ranges over Ω, the functions χ^ω turn out to be all the extreme characters of $U(\infty)$ [26,33,35].

Equipping $\mathbb{R}^\infty \times \mathbb{R}^\infty \times \mathbb{R}^\infty \times \mathbb{R}^\infty \times \mathbb{R} \times \mathbb{R}$ with the product topology induces a topology on Ω. For any fixed $U \in U(\infty)$, $\chi^\omega(U)$ is a continuous function of ω. For any character χ of $U(\infty)$, there exists a unique Borel probability measure P on Ω such that

$$\chi(U) = \int_\Omega \chi^\omega(U)\, dP,$$

see [29, Theorem 9.1]. This measure is called the *spectral measure* of χ.

The extreme characters of $U(\infty)$ can be approximated by χ^λ with growing signatures λ. To state this precisely we need more notation.

Represent a signature λ as a pair of Young diagrams (λ^+, λ^-), where λ^+ consists of positive λ_i's and λ^- consists of negative λ_i's. Zeroes can go in either of the two:

$$\lambda = \left(\lambda_1^+, \lambda_2^+, \ldots, -\lambda_2^-, -\lambda_1^-\right).$$

Let $d(\cdot)$ denote the number of diagonal boxes of a Young diagram and set $d^+ = d(\lambda^+)$ and $d^- = d(\lambda^-)$. Recall that the Frobenius coordinates p_i, q_i of a Young diagram λ are defined by

$$p_i = \lambda_i - i, \qquad q_i = (\lambda')_i - i, \quad 1 \leqslant i \leqslant d(\lambda),$$

where λ' is the transposed diagram, see e.g. [23].

The dimension of the irreducible representation of $U(N)$ indexed by a signature $\lambda = (\lambda_1, \ldots, \lambda_N)$ is given by Weyl's formula:

$$\dim_N \lambda = \chi^\lambda(1, \ldots, 1) = \prod_{1 \leqslant i < j \leqslant N} \frac{\lambda_i - i - \lambda_j + j}{j - i}.$$

Define the *normalized* irreducible characters by

$$\tilde{\chi}^\lambda = \frac{1}{\dim_N \lambda} \chi^\lambda.$$

Note that $\tilde{\chi}^\lambda(e) = 1$.

Given a sequence $\{f_N\}$ of functions on $U(N)$, we say that f_N's *approximate* a function f on $U(\infty)$ if for any fixed N_0, the restrictions of the functions f_N (for $N \geqslant N_0$) to $U(N_0)$ uniformly tend, as $N \to \infty$, to the restriction of f to $U(N_0)$. We have the following approximation theorem:

Theorem 2.1. *Let χ be the extreme character corresponding to $(\alpha^\pm, \beta^\pm, \gamma^\pm) \in \Omega$. Let $\{\lambda(n)\}$ be a sequence of signatures of length n with Frobenius coordinates $p_i^\pm(n), q_i^\pm(n)$. Then the functions $\tilde{\chi}^{\lambda(n)}$ approximate χ iff*

$$\lim_{n\to\infty} \frac{p_i^\pm(n)}{n} = \alpha_i^\pm, \qquad \lim_{n\to\infty} \frac{q_i^\pm(n)}{n} = \beta_i^\pm, \qquad \lim_{n\to\infty} \frac{|(\lambda(n))^\pm|}{n} = \delta^\pm$$

for all i.

Proof. This theorem is due to Vershik and Kerov [33]. See [26] for a detailed proof. □

Let $\mathbb{GT}_N$ be the set of all signatures of length N and set $\mathbb{GT} = \bigcup_N \mathbb{GT}_N$. Turn $\mathbb{GT}$ into a graph by drawing an edge between signatures $\lambda \in \mathbb{GT}_N$ and $\mu \in \mathbb{GT}_{N+1}$ if λ and μ satisfy the branching relation $\lambda \prec \mu$, where $\lambda \prec \mu$ means that $\mu_1 \leqslant \lambda_1 \leqslant \mu_2 \leqslant \lambda_2 \leqslant \cdots \leqslant \lambda_N \leqslant \mu_{N+1}$. $\mathbb{GT}$ is also known as the *Gelfand–Tsetlin graph*.

Each character of $U(\infty)$ defines a probability measure P_N on $\mathbb{GT}_N$. If we restrict the extreme character χ^ω to $U(N)$, we can write

$$\chi^\omega|_{U(N)} = \sum_{\lambda \in \mathbb{GT}_N} P_N(\lambda)\tilde{\chi}^\lambda. \tag{2}$$

Definition 2.2. The measure P_N corresponding to the extreme character with $\alpha^\pm = \beta^\pm = 0$ and arbitrary $\gamma^\pm \geqslant 0$ will be called the Nth level Plancherel measure with parameters $\gamma^\pm$. Denote it by $P_N^{\gamma^+,\gamma^-}$.

The choice of the term is explained by the analogy with the infinite symmetric group $S(\infty)$. The extreme characters of $S(\infty)$ are parameterized by

$$\left\{(\alpha,\beta,\gamma) \in \mathbb{R}_+^\infty \times \mathbb{R}_+^\infty \times \mathbb{R}_+;\ \sum(\alpha_i+\beta_i)+\gamma = 1\right\}.$$

The measure on partitions of n obtained from the character with $\alpha_i = \beta_i = 0, \gamma = 1$, similarly to the measure P_N above, assigns the weight $(\dim\lambda)^2/n!$ to a partition λ and is commonly called the Plancherel measure. Here $\dim\lambda$ is the dimension of the irreducible representation of S_n corresponding to λ.

Let χ be a character of $U(\infty)$ and let P and P_N be its corresponding decomposing measures on Ω and $\mathbb{GT}_N$. For any N, embed $\mathbb{GT}_N$ into Ω by sending λ to $(a^+, a^-, b^+, b^-, c^+, c^-)$ where

$$a_i^\pm = \frac{p_i^\pm}{N}, \qquad b_i^\pm = \frac{q_i^\pm}{N}, \qquad c^\pm = \frac{|\lambda^\pm|}{N}.$$

Define a probability measure $\underline{P}_N$ on Ω to be the pushforward of P_N under this embedding. Then $\underline{P}_N$ weakly converges to P as $N \to \infty$ [29, Theorem 10.2].

This implies that as $N \to \infty$, the Plancherel measures $P_N^{\gamma^+,\gamma^-}$ converge to the delta measure at $\omega = (\alpha_i^\pm = \beta_i^\pm = 0, \gamma^+, \gamma^-)$, that is, the row and column lengths for $\lambda^\pm$ distributed according to $P_N^{\gamma^+,\gamma^-}$ grow sublinearly in N.

The main goal of this paper is to study the asymptotic behavior of the signatures distributed according to the Plancherel measures $P_N^{\gamma^+,\gamma^-}$ as $N \to \infty$. We will also study a more general object: the corresponding probability measures on objects called paths in $\mathbb{GT}$.

A *path* in $\mathbb{GT}$ is an infinite sequence $t = (t_1, t_2, \ldots)$ such that $t_i \in \mathbb{GT}_i$ and $t_i \prec t_{i+1}$. Let $\mathcal{T}$ be the set of all paths.

We also have *finite paths*, which are sequences $\tau = (\tau_1, \tau_2, \ldots, \tau_N)$ such that $\tau_i \in \mathbb{GT}_i$ and $\tau_1 \prec \tau_2 \prec \cdots \prec \tau_N$. The set of all paths of length N is denoted by $\mathcal{T}_N$. For each finite path $\tau \in \mathcal{T}_N$, let C_τ be the set

$$C_\tau = \left\{t \in \mathcal{T}\colon\ (t_1, t_2, \ldots, t_N) = \tau\right\}.$$

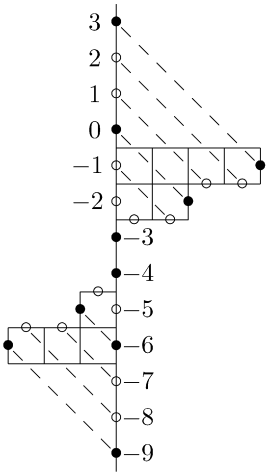

Fig. 1. Black dots represent points in the configuration and white dots represent points not in the configuration.

A character χ of $U(\infty)$ also defines a probability measure M^χ on $\mathcal{T}$ which can be specified by setting

$$M^\chi(C_\tau) = \frac{P_N(\lambda)}{\dim_N \lambda}, \tag{3}$$

where P_N is as above and τ is an arbitrary finite path ending at λ, see [29, Section 10] for details. In particular, any $\omega \in \Omega$ defines a measure on $\mathcal{T}$ via the corresponding extreme character χ^ω. If ω satisfies $\alpha_i^\pm = \beta_i^\pm = 0$ with arbitrary $\gamma^\pm$, then let P^{γ^+,γ^-} denote this measure.

3. Plancherel measures as determinantal point processes

In order to analyze $P_N^{\gamma^+,\gamma^-}$ and P^{γ^+,γ^-}, it is convenient to represent signatures as finite point configurations (subsets) in one-dimensional lattice. Assign to each signature $\lambda \in \mathbb{GT}_N$ a point configuration $\mathcal{L}(\lambda) \subset \mathbb{Z}$ by

$$\lambda = (\lambda_1, \dots, \lambda_N) \mapsto \mathcal{L}(\lambda) = \{\lambda_1 - 1, \dots, \lambda_N - N\}.$$

The pushforward of $P_N^{\gamma^+,\gamma^-}$ under this map is a measure on subsets of $\mathbb{Z}$, that is, a random point process on $\mathbb{Z}$. See Appendix A for general information on point processes. Denote this point process by $\mathcal{P}_N^{\gamma^+,\gamma^-}$. The map $\lambda \mapsto \mathcal{L}(\lambda)$ can be seen visually. For example, if $\lambda = (4, 2, 0, 0, -1, -3)$, then $\mathcal{L}(\lambda) = \{3, 0, -3, -4, -6, -9\}$. See Fig. 1.

Just as $\lambda \mapsto \mathcal{L}(\lambda)$ defines a map from $\mathbb{GT}_n$ to the set of subsets of $\mathbb{Z}$, we have a map from the set $\mathcal{T}$ of paths in the Gelfand–Tsetlin graph to subsets of $\mathbb{Z}_+ \times \mathbb{Z}$. Let $t = (t_1 \prec t_2 \prec \cdots)$ be a path in $\mathbb{GT}$. Each t_i is a signature of length i which will be written as $\lambda^{(i)} = (\lambda_1^{(i)}, \lambda_2^{(i)}, \dots, \lambda_i^{(i)})$. Then map t to

$$\mathcal{L}(t) = \left\{\left(i, \lambda_j^{(i)} - j\right)\colon\ 1 \leqslant i < \infty,\ 1 \leqslant j \leqslant i\right\} \subset \mathbb{Z}_+ \times \mathbb{Z}.$$

The pushforward of P^{γ^+,γ^-} under this map will be denoted by $\mathcal{P}^{\gamma^+,\gamma^-}$. This is a random point process on $\mathbb{Z}_+ \times \mathbb{Z}$.

Let us now state the main theorem of this section.

Theorem 3.1. *The point process $\mathcal{P}^{\gamma^+,\gamma^-}$ is determinantal. Let $K(n_i, x_i; n_j, x_j)$ denote its correlation kernel. If $n_1 \geqslant n_2$, then*

$$K(n_1, x_1; n_2, x_2) = \left(\frac{1}{2\pi i}\right)^2 \oint \oint \frac{e^{\gamma^- u + \gamma^+ u^{-1}} u^{x_1} (1-u)^{n_1}}{e^{\gamma^- w + \gamma^+ w^{-1}} w^{1+x_2} (1-w)^{n_2}} \frac{du\, dw}{u-w}.$$

If $n_1 < n_2$, then

$$\begin{aligned} K(n_1, x_1; n_2, x_2) = &-\frac{1}{2\pi i} \oint \frac{z^{x_1 - x_2 - 1}}{(1-z)^{n_2 - n_1}} dz \\ &+ \left(\frac{1}{2\pi i}\right)^2 \oint \oint \frac{e^{\gamma^- u + \gamma^+ u^{-1}} u^{x_1} (1-u)^{n_1}}{e^{\gamma^- w + \gamma^+ w^{-1}} w^{1+x_2} (1-w)^{n_2}} \frac{du\, dw}{u-w}. \end{aligned} \tag{4}$$

In these expressions, u is integrated over $|u| = r < 1$ and w is integrated over $|w-1| = \epsilon < 1-r$ and z is integrated over $|z| = r < 1$.

Let $\mathcal{P}_{\Delta}^{\gamma^+,\gamma^-}$ be the image of $\mathcal{P}^{\gamma^+,\gamma^-}$ under the particle-hole involution (see Appendix A for definitions).

Corollary 3.2. *The point process $\mathcal{P}_{\Delta}^{\gamma^+,\gamma^-}$ is determinantal. Let $K_{\Delta}(n_i, x_i; n_j, x_j)$ denote its correlation kernel. If $n_1 > n_2$, then*

$$K_{\Delta}(n_1, x_1; n_2, x_2) = -\left(\frac{1}{2\pi i}\right)^2 \oint \oint \frac{e^{\gamma^- u + \gamma^+ u^{-1}} u^{x_1} (1-u)^{n_1}}{e^{\gamma^- w + \gamma^+ w^{-1}} w^{1+x_2} (1-w)^{n_2}} \frac{du\, dw}{u-w}.$$

If $n_1 \leqslant n_2$, then

$$\begin{aligned} K_{\Delta}(n_1, x_1; n_2, x_2) = &\frac{1}{2\pi i} \oint \frac{z^{x_1 - x_2 - 1}}{(1-z)^{n_2 - n_1}} dz \\ &- \left(\frac{1}{2\pi i}\right)^2 \oint \oint \frac{e^{\gamma^- u + \gamma^+ u^{-1}} u^{x_1} (1-u)^{n_1}}{e^{\gamma^- w + \gamma^+ w^{-1}} w^{1+x_2} (1-w)^{n_2}} \frac{du\, dw}{u-w}. \end{aligned} \tag{5}$$

In these expressions, u is integrated over $|u| = r < 1$ and w is integrated over $|w-1| = \epsilon < 1-r$ and z is integrated over $|z| = r < 1$.

Proof. The corollary follows immediately from Proposition A and the fact that

$$\delta_{x_1 = x_2} = \frac{1}{2\pi i} \oint_{|z|=r} \frac{z^{x_1 - x_2 - 1}}{(1-z)^{n_2 - n_1}} dz$$

for $n_1 = n_2$. Note that in Theorem 3.1 the two cases for the kernel are $n_1 \geqslant n_2$ and $n_1 < n_2$, while in Corollary 3.2 the two cases are $n_1 > n_2$ and $n_1 \leqslant n_2$. □

Remark. Let $\bar{K}(n_1, x_1; n_2, x_2)$ and $\bar{K}_\Delta(n_1, x_1; n_2, x_2)$ denote the correlation kernels of $\mathcal{P}^{\gamma^-,\gamma^+}$ and $\mathcal{P}_\Delta^{\gamma^-,\gamma^+}$, respectively ($\gamma^+$ and γ^- switched places). These kernels are real-valued, and they are non-symmetric. However, the substitutions $u \mapsto u^{-1}$, $w \mapsto w^{-1}$ and further deformation of the contours show that

$$(-1)^{n_1-n_2} K(n_1, -x_1 - n_1 - 1; n_2, -x_2 - n_2 - 1) = \bar{K}(n_1, x_1; n_2, x_2),$$
$$(-1)^{n_1-n_2} K_\Delta(n_1, -x_1 - n_1 - 1; n_2, -x_2 - n_2 - 1) = \bar{K}_\Delta(n_1, x_1; n_2, x_2).$$

This can be understood independently. Switching γ^+ and γ^- corresponds to switching λ^+ and λ^- in a signature λ. In terms of $\mathcal{L}(\lambda)$, this corresponds to replacing x_i with $-x_i - n_i - 1$. For example, consider $\lambda = (4, 2, 0, 0, -1, -3)$ from Fig. 1. Switching λ^+ and λ^- gives $\bar{\lambda} = (3, 1, 0, 0, -2, -4)$. Then $\mathcal{L}(\bar{\lambda}) = \{2, -1, -3, -4, -7, -10\}$, which can be obtained from $\mathcal{L}(\lambda)$ by replacing x_i with $-x_i - 6 - 1$.

Remark. The arguments below actually prove a more general statement. If we define a point process of $\mathbb{Z}_+ \times \mathbb{Z}$ similarly to $\mathcal{P}^{\gamma^+,\gamma^-}$, but starting from an extreme character of $U(\infty)$ with arbitrary parameters $(\alpha_i^\pm, \beta_i^\pm, \gamma^\pm)$, then this process is determinantal and its kernel has a similar form. The only change is replacing $E(z)$ below by $f_0(z)$ from Eq. (1).

In what follows we use the notation

$$E(z) = e^{\gamma^+(z-1)+\gamma^-(z^{-1}-1)} = e^{-\gamma^+-\gamma^-} e^{\gamma^+ z+\gamma^- z^{-1}}.$$

Lemma 3.3. *Suppose* $\lambda = (\lambda_1, \lambda_2, \ldots, \lambda_N) \in \mathbb{GT}_N$. *Write* x_k *for* $\lambda_k - k$. *Then*

$$P_N^{\gamma^+,\gamma^-}(\lambda) = \frac{1}{1!2!\ldots(N-1)!} \cdot \det\bigl[f_j(x_k)\bigr]_{1\leqslant j,k\leqslant N} \det\bigl[g_j(x_k)\bigr]_{1\leqslant j,k\leqslant N}$$

where

$$f_j(x_k) = \frac{1}{2\pi i} \oint_{|u|=1} E(u) u^{-1-x_k-j}\, du, \quad 1 \leqslant j \leqslant N, \tag{6}$$

$$g_j(x_k) = x_k^{j-1}, \quad 1 \leqslant j \leqslant N. \tag{7}$$

Proof. Writing $E(u) = \sum_{l=-\infty}^{\infty} c(l) u^l$ and integrating $E(u)u^k$ over the unit circle, we can solve for c to get

$$c(l) = \frac{1}{2\pi i} \oint_{|u|=1} E(u) u^{-1-l}\, du.$$

Set $\omega = (\alpha_i^{\pm} = \beta_i^{\pm} = 0, \gamma^+, \gamma^-)$. For $U \in U(N)$ with spectrum $u_1, \dots, u_N$, we can write $\chi^{\omega}(U) = E(u_1) \dots E(u_N)$. Recall that $P_N^{\gamma^+,\gamma^-}$ is defined by (2). Using [29, Lemma 6.5], we can express $\chi^{\omega}|_{U(N)}$ as $\sum_{\lambda \in \mathbb{GT}_N} c(\lambda)\chi^{\lambda}$, where

$$c(\lambda) = c(\lambda_1, \dots, \lambda_N) = \det\bigl[c(\lambda_k - k + j)\bigr]_{1 \leqslant j,k \leqslant N}.$$

Set $f_j(x_k) = c(x_k + j)$. Since $\chi^{\lambda} = \tilde{\chi}^{\lambda} \cdot \dim_N \lambda$, with

$$\dim_N \lambda = \prod_{1 \leqslant i < j \leqslant N} \frac{\lambda_i - i - \lambda_j + j}{j - i} = \frac{1}{1!2! \dots (N-1)!} \cdot \prod_{1 \leqslant i < j \leqslant N} \bigl((\lambda_i - i) - (\lambda_j - j)\bigr),$$

we get the additional Vandermonde determinant $\det[(\lambda_k - k)^{j-1}] = \det[x_k^{j-1}]$. □

Remark. Observe that the argument above and (3) imply that

$$P^{\gamma^+,\gamma^-}(C_\tau) = \det\bigl[f_j(x_k)\bigr]_{1 \leqslant j,k \leqslant N}.$$

To state the next result we need slightly different notation. Let

$$\mathcal{P}^{\gamma^+,\gamma^-}\bigl(\bigl\{x_k^{(n)}\colon\ 1 \leqslant n \leqslant N,\ 1 \leqslant k \leqslant n\bigr\}\bigr) = P^{\gamma^+,\gamma^-}(C_\tau)$$

if there exists a path $\tau = (\lambda^{(1)} \prec \cdots \prec \lambda^{(n)})$ such that

$$\lambda^{(n)} = \bigl(x_1^{(n)} + 1, x_2^{(n)} + 2, \dots, x_n^{(n)} + n\bigr),$$

and $\mathcal{P}^{\gamma^+,\gamma^-}(\{x_k^{(n)}\}) = 0$ otherwise.

Proposition 3.4. *Let $\{x_k^{(n)}\colon\ 1 \leqslant n \leqslant N,\ 1 \leqslant k \leqslant n\}$ be arbitrary integers satisfying $x_k^{(n)} \geqslant x_{k+1}^{(n)}$ for all n, k. Then*

$$\begin{aligned}&\mathcal{P}^{\gamma^+,\gamma^-}\bigl(\bigl\{x_k^{(n)}\colon\ 1 \leqslant n \leqslant N,\ 1 \leqslant k \leqslant n\bigr\}\bigr)\\ &\quad= \frac{1}{1!2! \dots (N-1)!} \cdot \prod_{n=1}^{N-1} \det\bigl[\phi_n\bigl(x_i^{(n)}, x_j^{(n+1)}\bigr)\bigr]_{1 \leqslant i,j \leqslant n+1} \det\bigl[f_i\bigl(x_j^{(N)}\bigr)\bigr]_{1 \leqslant i,j \leqslant N}\end{aligned}$$

where $x_{n+1}^{(n)}$ are "virtual" variables,[1] *and ϕ_n is defined by*

$$\phi_n(x, y) := \begin{cases} 1 & \text{if } x \leqslant y,\\ 1 & x \text{ "virtual,"}\\ 0 & \text{otherwise.}\end{cases}$$

[1] One can think of "virtual" variables as being equal to negative infinity.

Proof. By the remark after 3.3, it suffices to prove that $\prod \det[\phi_n]$ acts as an indicator function. It takes the value of 1 if $\lambda^{(1)} \prec \lambda^{(2)} \prec \cdots \prec \lambda^{(N)}$ and 0 otherwise, where

$$\lambda^{(n)} = \big(x_1^{(n)} + 1, \ldots, x_n^{(n)} + n\big).$$

If $\lambda^{(1)} \prec \lambda^{(2)} \prec \cdots \prec \lambda^{(N)}$, so that $x_1^{(n+1)} \geqslant x_1^{(n)} > x_2^{(n+1)} \geqslant x_2^{(n)} > \cdots \geqslant x_n^{(n)} > x_{n+1}^{(n+1)}$ for each n, then

$$\phi_n\big(x_i^{(n)}, x_j^{(n+1)}\big) = \begin{cases} 1 & \text{if } j \leqslant i, \\ 0 & \text{if } i < j. \end{cases}$$

So $\det[\phi_n] = 1$ for each n.

Conversely, suppose that $\prod \det[\phi_n] = 1$, so that $\det[\phi_n] \neq 0$ for each n. Notice that the matrix $[\phi_n(x_i^{(n)}, x_j^{(n+1)})]$ consists entirely of zeroes and ones. Also notice that the number of ones in the kth column is greater than or equal to the number of ones in the jth column for $k < j$. Additionally, if the (i, j) entry is zero then so is the $(i - 1, j)$ entry. Since the determinant is nonzero, this means that no two columns are equal, so each column must have a different number of ones, so the (i, j) entry is 1 if $j \leqslant i$ and 0 if $i < j$. This says exactly that $\lambda^{(1)} \prec \lambda^{(2)} \prec \cdots \prec \lambda^{(N)}$, and each determinant in the product is equal to 1. □

We can now prove Theorem 3.1.

Proof of Theorem 3.1. For computational purposes, it is actually easier to consider

$$\phi_n(x, y) := \begin{cases} \theta_n^{x-y} & \text{if } x \leqslant y, \\ \theta_n^{-y} & x \text{ “virtual,”} \\ 0 & \text{otherwise} \end{cases}$$

with mutually distinct θ_n's and then take $\theta_n \to 1$. It is also convenient to denote $\theta_0 = 1$. We will assume that $|\theta_n| > |\theta_{n-1}| > 1$ for all n. Notice that $\det[f_i(x_j^{(N)})]$ only depends on the linear span of $f_1, \ldots, f_N$ (up to a constant), so redefine

$$f_j(x) = \frac{1}{2\pi i} \oint_{|u|=\text{const}} E(u) u^{-2-x} p_{j-1}\big(u^{-1}\big)\, du, \quad \text{where}$$

$$p_{j-1}(x) = (\theta_0 - x) \ldots \widehat{(\theta_{j-1} - x)} \ldots (\theta_{N-1} - x) = \prod_{k=0, k\neq j-1}^{N-1} (\theta_k - x).$$

The rest of the proof is a direct application of Lemma 3.4 of [7], where we use the notation $\Psi_{N-j}^N = f_j$. For readers' convenience, this lemma is discussed in Appendix B. Although the statement holds for signed measures, the measures considered below are actually positive as long as all θ_k's are positive.

All series below converge exponentially fast as long as θ_k's are bounded away from the unit disc.

Taking the Fourier Transform of ϕ_n, we obtain

$$\phi_n(x,y) = \frac{1}{2\pi i}\oint_{|z|=1} F_n(z) z^{x-y-1}\,dz,$$

$$\phi^{(n_1,n_2)}(x,y) = \frac{1}{2\pi i}\oint_{|z|=1} F_{n_1}(z)\dots F_{n_2-1}(z) z^{x-y-1}\,dz \tag{8}$$

where $F_n(z) = (1-\theta_n^{-1}z)^{-1}$ and $n_1 < n_2$. We also agree that $\phi^{(n_1,n_2)} \equiv 0$ if $n_1 \geqslant n_2$. In case x is a "virtual" variable (which is denoted by virt), then

$$\begin{aligned}\phi^{(n_1,n_2)}(\text{virt},y) &= \sum_{m\in\mathbb{Z}} \phi_{n_1}(\text{virt},m)\phi^{(n_1+1,n_2)}(m,y)\\ &= \frac{\theta_{n_1}^{-y}}{2\pi i}\oint F_{n_1+1}(z)\dots F_{n_2-1}(z)\frac{dz}{z-\theta_{n_1}}\\ &= \theta_{n_1}^{-y} F_{n_1+1}(\theta_{n_1})\dots F_{n_2-1}(\theta_{n_1}),\end{aligned}$$

where the contour integral is taken over $|z| = r$ for some $|\theta_{n_1}| < r < |\theta_{n_1+1}|$.

This allows us to calculate the matrix M (cf. Lemma 3.4 of [7] or Appendix B):

$$\begin{aligned}M_{ij} &= \big(\phi^{(i-1,N)} * \Psi^N_{N-j}\big)(\text{virt}) = \sum_{y\in\mathbb{Z}} \phi^{(i-1,N)}(\text{virt},y)\Psi^N_{N-j}(y)\\ &= \sum_{y\in\mathbb{Z}} \theta_{i-1}^{-y} F_i(\theta_{i-1})\dots F_{N-1}(\theta_{i-1})\cdot\frac{1}{2\pi i}\oint_{|u|=1} E(u)u^{-2-y}p_{j-1}\big(u^{-1}\big)\,du\\ &= -F_i(\theta_{i-1})\dots F_{N-1}(\theta_{i-1})\frac{1}{2\pi i}\oint E(u)u^{-2}p_{j-1}\big(u^{-1}\big)\frac{u\theta_{i-1}}{1-u\theta_{i-1}}\,du\\ &= F_i(\theta_{i-1})\dots F_{N-1}(\theta_{i-1})E\big(\theta_{i-1}^{-1}\big)p_{j-1}(\theta_{i-1})\theta_{i-1},\end{aligned}$$

where the second contour integral is taken over an annulus of radii r and 1 for some $r < |\theta_{i-1}|^{-1}$.

Notice that M is diagonal because $p_{j-1}(\theta_{i-1}) = 0$ unless $i = j$. We have one more preliminary calculation (cf. [7, formula (3.22)]):

$$\begin{aligned}\Psi^n_{n-j}(x) &= \sum_{y\in\mathbb{Z}} \phi^{(n,N)}(x,y)\Psi^N_{N-j}(y)\\ &= \left(\frac{1}{2\pi i}\right)^2 \oint_{|z|=1} F_n(z)\dots F_{N-1}(z)z^{x-1}\,dz \oint_{|u|=R>1} E(u)u^{-2}p_{j-1}\big(u^{-1}\big)\sum_{y\geqslant x}(zu)^{-y}\,du\\ &= \left(\frac{1}{2\pi i}\right)^2 \oint_{|z|=1} F_n(z)\dots F_{N-1}(z)z^{-1}\,dz \oint_{|u|=R>1} E(u)u^{-2-x}p_{j-1}\big(u^{-1}\big)\frac{du}{1-(zu)^{-1}}\end{aligned}$$

$$= \frac{1}{2\pi i} \oint_{|u|=1} F_n\big(u^{-1}\big) \dots F_{N-1}\big(u^{-1}\big) E(u) u^{-2-x} p_{j-1}\big(u^{-1}\big)\, du.$$

We can now calculate K according to [7, formula (3.26)]. For $n_1 < n_2$,

$$\begin{aligned}
&K(n_1, x_1; n_2, x_2) + \phi^{(n_1,n_2)}(x_1, x_2) \\
&\quad = \sum_{k=1}^{n_2} \Psi^{n_1}_{n_1-k}(x_1) \sum_{l=1}^{N} \big[M^{-1}\big]_{k,l} \big(\phi_{l-1} * \phi^{(l,n_2)}\big)\big(x_l^{l-1}, x_2\big) \\
&\quad = \sum_{k=1}^{n_2} \big[M^{-1}\big]_{kk} \Psi^{n_1}_{n_1-k}(x_1) \phi^{(k-1,n_2)}(\mathrm{virt}, x_2) \\
&\quad = \frac{1}{2\pi i} \oint_{|u|=1} F_{n_1}\big(u^{-1}\big) \dots F_{N-1}\big(u^{-1}\big) E(u) u^{-2-x_1} \\
&\qquad \times \sum_{k=1}^{n_2} \frac{\theta_{k-1}^{-x_2} F_k(\theta_{k-1}) \dots F_{n_2-1}(\theta_{k-1}) p_{k-1}(u^{-1})}{F_k(\theta_{k-1}) \dots F_{N-1}(\theta_{k-1}) E(\theta_{k-1}^{-1}) p_{k-1}(\theta_{k-1}) \theta_{k-1}}\, du \\
&\quad = \frac{1}{2\pi i} \oint_{|u|=1} F_{n_1}\big(u^{-1}\big) \dots F_{N-1}\big(u^{-1}\big) E(u) u^{-2-x_1} \\
&\qquad \times \sum_{k=1}^{n_2} \frac{\theta_{k-1}^{-x_2} p_{k-1}(u^{-1})}{F_{n_2}(\theta_{k-1}) \dots F_{N-1}(\theta_{k-1}) E(\theta_{k-1}^{-1}) p_{k-1}(\theta_{k-1}) \theta_{k-1}}\, du \\
&\quad = \frac{1}{2\pi i} \oint_{|u|=1} u^{-2-x_1} \\
&\qquad \times \left(\sum_{k=1}^{n_1} \frac{\theta_{n_1} \dots \theta_{N-1} E(u) \prod_{l=0, l\neq k-1}^{n_1-1} (\theta_l - u^{-1})}{\theta_{n_2} \dots \theta_{N-1} E(\theta_{k-1}^{-1}) \prod_{l=0, l\neq k-1}^{n_2-1} (\theta_l - \theta_{k-1})} \theta_{k-1}^{-1-x_2} \right. \\
&\qquad \left. + \sum_{k=1+n_1}^{n_2} \frac{\theta_{n_1} \dots \theta_{N-1} E(u) \prod_{l=0}^{n_1-1} (\theta_l - u^{-1})}{(\theta_{k-1} - u^{-1}) \theta_{n_2} \dots \theta_{N-1} E(\theta_{k-1}) \prod_{l=0, l\neq k-1}^{n_2-1} (\theta_l - \theta_{k-1})} \theta_{k-1}^{-1-x_2} \right) du
\end{aligned}$$

and for $n_1 \geqslant n_2$ the last sum is omitted.

We can write the expression in parentheses as a contour integral that goes around all the θ_j, so we get

$$\left(\frac{1}{2\pi i}\right)^2 \oint_{|u|=r^{-1}>1} \oint_{|z-1|=\epsilon} \frac{(\theta_0 - u^{-1}) \dots (\theta_{n_1-1} - u^{-1}) E(u) u^{-2-x_1}}{(\theta_0 - z) \dots (\theta_{n_2-1} - z) E(z^{-1}) z^{1+x_2}} \frac{\theta_{n_2} \dots \theta_{n_1-1}}{(u^{-1} - z)}\, du\, dz,$$

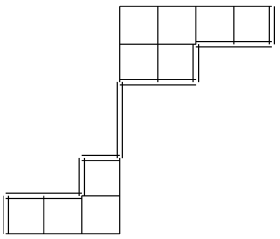

Fig. 2. The double lines show the boundary.

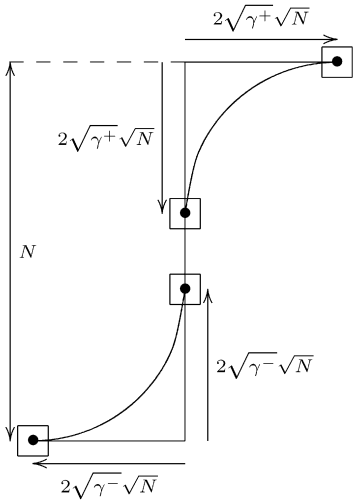

Fig. 3. A visual representation.

assuming that $|\theta_n - 1| < \epsilon$ for all n. Substituting $u \to u^{-1}$ gives

$$\left(\frac{1}{2\pi i}\right)^2 \oint_{|u|=r<1} \oint_{|z-1|=\epsilon} \frac{(\theta_0 - u)\dots(\theta_{n_1-1} - u)E(u^{-1})u^{x_1}}{(\theta_0 - z)\dots(\theta_{n_2-1} - z)E(z^{-1})z^{1+x_2}} \frac{\theta_{n_2}\dots\theta_{n_1-1}}{(u-z)}\,du\,dz.$$

There is also the term $-\phi^{(n_1,n_2)}(x_1, x_2)$ from (8), which equals

$$-\left(\frac{1}{2\pi i}\right)^2 \oint_{|z|=\text{const}<1} \frac{z^{x_1-x_2-1}}{(1-\theta_{n_1}^{-1}z)\dots(1-\theta_{n_2-1}^{-1}z)}\,dz$$

if $n_1 < n_2$ and 0 if $n_1 \geqslant n_2$. Finally, taking all the θ_j to be 1 yields the result. □

4. Limits

4.1. Limit shape

Represent $\lambda \in \mathbb{GT}_N$ as a pair of Young diagrams (λ^+, λ^-). Fig. 2 gives an example with $\lambda = (4, 2, 0, 0, -1, -3)$, $\lambda^+ = (4, 2)$, $\lambda^- = (3, 1)$. We have the following conjecture:

Regard $\lambda \in \mathbb{GT}_N$ as random objects on the probability space $(\mathbb{GT}_N, P_N^{\gamma^+,\gamma^-})$. As $N \to \infty$, the boundaries of the two Young diagrams, scaled by $N^{-1/2}$, tend to (nonrandom) limit curves. Both limit curves coincide with the Vershik–Kerov–Logan–Shepp limit curve arising from the Plancherel measure on symmetric groups (see [22,32,33]).

Our results strongly suggest that this statement holds, see Section 3.2.

The conditions $\alpha_i^{\pm} = \beta_i^{\pm} = 0$ tell us that for fixed $\gamma^{\pm}$ every row and column length grows sublinearly in N (see the end of Section 1). Furthermore, since $\gamma^{\pm}$ correspond to the area of the Young diagrams $\lambda^{\pm}$ (see Section 1), this suggests a scaling of $N^{-1/2}$. See Fig. 3.

Furthermore, we see from Fig. 1 that vertical segments of the boundary correspond to points in the configuration, while horizontal segments correspond to points not in the configuration. This implies that the first correlation function $\rho_1(x)$ (also known as the density function) corresponds to the density of vertical segments in the boundary. For example, in between the two curves in Fig. 3, the vertical segments are densely packed, so $\rho_1(x)$ should converge to 1. Above the top curve (the boundary of λ^+) and below the bottom curve (the boundary of λ^-), the horizontal segments are densely packed, so $\rho_1(x)$ should converge to 0. We will see that this is indeed the case.

Notice that near the edges of the Young diagrams (the boxes in Fig. 3), the probability of finding a vertical segment tends to 0 or 1. This means that the vertical segments (or horizontal segments) become so rare that they occur infinitely far away from each other. In other words, for any fixed k, the differences $\lambda_k^{\pm} - \lambda_{k+1}^{\pm}$ and $(\lambda^{\pm})'_k - (\lambda^{\pm})'_{k+1}$ both go to infinity as $N \to \infty$. In fact, we find that $\lambda_k^{\pm} - \lambda_{k+1}^{\pm}$ and $(\lambda^{\pm})'_k - (\lambda^{\pm})'_{k+1}$ are of order $N^{1/6}$. The limiting distribution of $\lambda_k^{\pm} - \lambda_{k+1}^{\pm}$ or $(\lambda^{\pm})'_k - (\lambda^{\pm})'_{k+1}$ normalized by $N^{1/6}$ is referred to as the *edge scaling limit*. We will later prove that the well-known Airy determinantal point process appears in the edge limits. On the other hand, if we zoom in at any other point on the limit curves, the behavior there is different. At these points, the differences between consecutive rows and columns stay finite. Their limiting distributions are described by the *bulk limit*. We prove that it coincides with the discrete sine determinantal process. The limit density function in the bulk predicts the limit shape.

We should also consider what happens to the more general object—the corresponding measure on the set τ of paths in $\mathbb{GT}$ (see Section 1). Consider two signatures on such a path at levels n_1 and n_2. If $n_1 - n_2$ stays bounded then the bulk and the edge limits of these two signatures are indistinguishable (the local point configurations are essentially the same). However, as $n_2 - n_1$ grows, we may see nontrivial joint distributions. It turns out that the proper level scaling in the bulk is $n_1 - n_2 \sim \sqrt{N}$ while at the edge it is $n_1 - n_2 \sim N^{2/3}$. We will compute the corresponding scaling limits of the correlation functions later.

It is also interesting to consider the case when the parameters $\gamma^{\pm}$ depend on N. If $\gamma^{\pm}$ depend on N in such a way that $\gamma^{\pm} N \to a > 0$, then the areas of the Young diagrams $\lambda^{\pm}$ stay finite. More precisely, we obtain two independent copies of the Poissonized Plancherel measure for symmetric groups.

Additionally, consider what happens when $\gamma^{\pm}$ depend on N in such a way that $\gamma^+/N \to a > 0$ and $\gamma^-/N \to b > 0$ as $N \to \infty$. The Young diagrams are now scaled by N^{-1}. Computing the asymptotics of the density function of the vertical segments of the boundary, we see that the new hypothetical limit shape (which is just the integral of the density function) depends on the values of a and b. See Fig. 4.

It turns out, see Theorem 4.6 below, that the edges of the limit curves (where the density function reaches values 0 or 1) correspond to the real roots of a fourth degree polynomial

$$Q_{a,b}(z) = p_0 + p_1\left(z + \frac{1}{2}\right) + p_2\left(z + \frac{1}{2}\right)^2 + p_3\left(z + \frac{1}{2}\right)^3 + 16\left(z + \frac{1}{2}\right)^4,$$

$$p_0 = 1 - 12(a+b) + 4\left(a^2 + b^2\right) + 184ab - 256ab(a+b) + 64ab(a-b)^2,$$

$$p_1 = 8(b-a)(7 - 2a - 2b + 16ab),$$

$$p_2 = 8\left(2(a+b)^2 - 10(a+b) - 1\right), \qquad p_3 = 32(b-a).$$

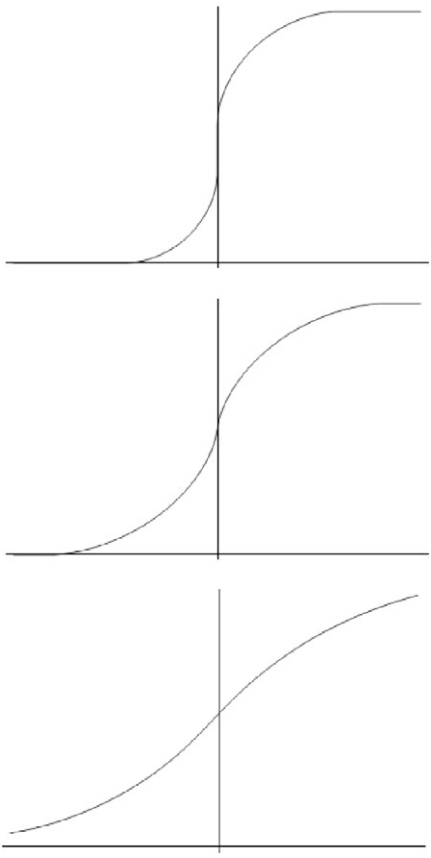

Fig. 4. The limit curves for various values of a and b. The top curve occurs when $a = \frac{1}{25}$, $b = \frac{1}{15}$, the middle curve occurs when $a = b = \frac{1}{8}$, the bottom curve occurs when $a = \frac{1}{4}$, $b = \frac{1}{3}$. In the top picture, the middle segment of the curve coincides with the vertical line. In the middle picture, the vertical line is tangent to the curve.

The expression $Q_{a,b}(c)$ is the discriminant of a simpler polynomial

$$R_{a,b,c}(z) = -bz^3 + (b - c - 1)z^2 + (c + a)z - a.$$

For small a and b, $Q_{a,b}$ has four real roots. As a and b increase, two of the real roots become closer until they merge into a double root. For larger values of a and b, $Q_{a,b}(z)$ has two real roots.

We will be able to find what values of a and b lead to $Q_{a,b}$ having exactly three distinct real roots (the middle root is a double root). This corresponds to the situation when the two limit curves just barely merge (see the middle image in Fig. 4). The correct scaling there is to let $(\lambda^{\pm})'_i - (\lambda^{\pm})'_{i+1} \sim N^{1/4}$ and $n_1 - n_2 \sim N^{1/2}$, which results in the Pearcey determinantal process appearing in the limit. At the other edges, letting $\lambda_i - \lambda_{i+1} \sim N^{1/3}$ or $(\lambda^{\pm})'_i - (\lambda^{\pm})'_{i+1}$ and $n_1 - n_2 \sim N^{2/3}$ results in the Airy process appearing. Away from the edges we still observe the bulk limit.

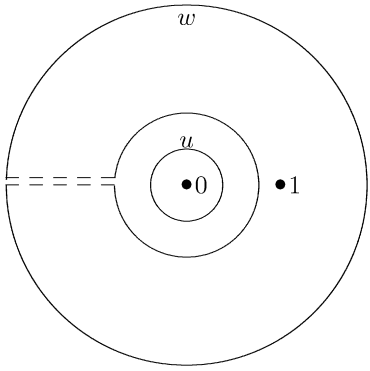

Fig. 5. Deformation of the contours.

We now proceed to computing the (scaling) limits of our determinantal point process $\mathcal{P}^{\gamma^+,\gamma^-}$ corresponding to the limit regimes described above.

4.2. Limits with $\gamma^{\pm} \propto 1/N$

Introduce the kernel $\mathbb{J}$ on $\mathbb{R}_+ \times \mathbb{Z}$ by

$$\mathbb{J}(s,x;t,y) = \left(\frac{1}{2\pi i}\right)^2 \oint\oint \frac{e^{u^{-1}-tu-w^{-1}+sw}}{w-u}\,\frac{du\,dw}{w^{x+1}u^{-y}}$$

where the w and u contours go counterclockwise around 0 in such a way that the w-contour contains the u-contour if $s \geqslant t$, and the w-contour is contained in the u-contour if $s < t$. This kernel for $s = t$ is equivalent to the discrete Bessel kernel $\mathbb{K}_{\mathrm{Bessel}}$, which appears when analyzing Plancherel measures for symmetric groups (see e.g., [25, §2.4]). Additionally, $\mathbb{J}$ is a special case of the kernel [10, (3.3)] corresponding to $\theta(t) = e^{-2t}$.

Theorem 4.1. *Let $x_1, \ldots, x_k$ be finite and constant. Let $n_1, \ldots, n_k$ and $\gamma^{\pm}$ depend on N in such a way that $n_j/N \to t_j > 0$ and $\gamma^{\pm} N \to a > 0$. Then as $N \to \infty$,*

$$\det\big[K(n_i, x_i; n_j, x_j)\big]_{1\leqslant i,j\leqslant k} \to \det\big[\mathbb{J}(at_i, x_i; at_j, x_j)\big]_{1\leqslant i,j\leqslant k}.$$

Proof. We use the integral representation for the kernel in Theorem 3.1.

We first focus our attention on the double integral in u and w. Since the integrand is holomorphic everywhere except at $u = 0$, $w = 1$, $w = u$ and $w = 0$, we can deform the contours of integration as shown in Fig. 5.

As $N \to \infty$, the integrand converges to 0 for $|w|$ large enough because $|1 - w| \gg |1 - u|$. Therefore we can ignore the outer half of the w contour. Then the contours of integration can be deformed to $|u| = a/N$ and $|w| = 2a/N$. Making the substitutions $u' = Nu/a$ and $w' = Nw/a$, the double integral is now

$$\frac{1}{(2\pi i)^2} \oint_{|u'|=1}\oint_{|w'|=2} \frac{e^{\gamma^+ u'^{-1}N/a + \gamma^- u' a/N}}{e^{\gamma^+ w'^{-1}N/a + \gamma^- w' a/N}}\,\frac{u'^{x_i}(1-u'a/N)^{n_i}}{w'^{x_j+1}(1-w'a/N)^{n_j}}\,\frac{du'\,dw'}{w'-u'}\left(\frac{N}{a}\right)^{x_j-x_i}$$

$$= \frac{1}{(2\pi i)^2} \oint_{|u'|=1} \oint_{|w'|=2} \frac{e^{u'^{-1}-at_i u'-w'^{-1}+at_j w'+O(1/N)}}{w'-u'} \frac{du\,dw}{u'^{-x_i} w'^{x_j+1}} (N/a)^{x_j-x_i}.$$

When taking the determinant, the term $(N/a)^{x_j-x_i}$ cancels. This gives the result.

Remark. Comparing this result to [8], we see that the distribution of λ^+ converges to the Poissonized Plancherel measure for the symmetric groups. By the symmetry $(\lambda^\pm \leftrightarrow \lambda^\mp, \gamma^\pm \leftrightarrow \gamma^\mp)$ the same is true for λ^-. On the other hand, a similar contour integral argument to the above shows that $K(n_i, x_i; n_j, -n_j - x_j - 1) \to 0$ as $N \to \infty$, which implies that λ^+ and λ^- are asymptotically independent. □

4.3. Bulk limits with $\gamma^\pm$ fixed

To state the next result, we need a definition. Given a complex number z_+ in the upper half plane, define

$$S_{z_+}(t_i - t_j; x_i - x_j) = \frac{1}{2\pi i} \int_{\overline{z_+}}^{z_+} u^{x_i-x_j-1} e^{(t_j-t_i)u}\,du.$$

If $t_i \geqslant t_j$, then the integration contour crosses $(0, \infty)$ but does not cross $(-\infty, 0)$. If $t_i < t_j$, then the integration contour crosses $(-\infty, 0)$ but not $(0, \infty)$. This kernel is one of the extensions of the discrete sine kernel constricted to [5]. A similar kernel appeared in [10]. It can be seen as a degeneration of the incomplete beta kernel, see Section 4.4.

The main theorem of this section is the following:

Theorem 4.2. *Let $x_1, \ldots, x_k$ and $n_1, \ldots, n_k$ all depend on N in such a way that $x_i - x_j$ is constant, $(n_j - N)/\sqrt{N} \to t_j \in \mathbb{R}$ and $x_i/\sqrt{N} \to c \in \mathbb{R}$ for all $1 \leqslant i, j \leqslant k$. Write z_+ for $(c + \sqrt{c^2 - 4\gamma^+})/2$. Then*

$$\lim_{N\to\infty} \det\big[K(n_i, x_i; n_j, x_j)\big]_{1\leqslant i,j\leqslant k} = \begin{cases} 0, & c \geqslant 2\sqrt{\gamma^+}, \\ 1, & c \leqslant -2\sqrt{\gamma^+}, \\ \det\big[S_{z_+}(t_i - t_j; x_i - x_j)\big]_{1\leqslant i,j\leqslant k}, & -2\sqrt{\gamma^+} < c < 2\sqrt{\gamma^+}. \end{cases}$$

Remark. Theorem 4.2 only makes a statement about the behavior around the top limit curve in Fig. 3. If we replace x_i with $-x_i - n_i - 1$ and γ^+ with γ^-, then by symmetry the same statement holds for the asymptotics around the lower Young diagram.

Corollary 4.3. *Let $\rho_1(N, x)$ be the density function of $\mathcal{P}_N^{\gamma^+,\gamma^-}$. Then $\lim_{N\to\infty} \rho_1(N, \alpha N + \beta N^{1/2})$ equals*

- *0, if $\alpha > 0$ or $\alpha < -1$ or $\alpha = 0, \beta \geqslant 2\sqrt{\gamma^+}$ or $\alpha = -1, \beta \leqslant -2\sqrt{\gamma^+}$,*

- 1 *if* $-1 \leqslant \alpha < 0$ *or* $\alpha = 0, \beta < -2\sqrt{\gamma^+}$ *or* $\alpha = -1, \beta \geqslant 2\sqrt{\gamma^+}$,
- $\frac{1}{\pi} \arccos(\frac{\beta}{2\sqrt{\gamma^+}})$ *if* $\alpha = 0, -2\sqrt{\gamma^+} < \beta < 2\sqrt{\gamma^+}$ *or* $\alpha = -1, -2\sqrt{\gamma^+} < \beta < 2\sqrt{\gamma^+}$.

Proof. The arguments are similar to those used for the analysis of Plancherel measures for the symmetric groups in [25].

For reasons that will later become clear, it is more convenient to analyze $N^{(x_i-x_j)/2} \times (\gamma^+)^{(x_j-x_i)/2} K(n_i, x_i; n_j, x_j)$. When taking the determinant

$$\det\bigl[N^{(x_i-x_j)/2}\bigl(\gamma^+\bigr)^{(x_j-x_i)/2} K(n_i, x_i; n_j, x_j)\bigr],$$

the term $N^{(x_i-x_j)/2}(\gamma^+)^{(x_j-x_i)/2}$ cancels out.

We use the integral representation for the kernel in Theorem 3.1. The conditions $n_i \geqslant n_j$ and $n_i < n_j$ translate to $t_i \geqslant t_j$ and $t_i < t_j$, respectively.

Just as in Theorem 4.1, we can deform the contours of integration as shown in Fig. 5.

As $N \to \infty$, the integrand converges to 0 for $|w|$ large enough because $|1-w| \gg |1-u|$. Therefore we can ignore the outer half of the w contour. Then the contours of integration can be deformed to $|u| = 1/\sqrt{N}$ and $|w| = 2/\sqrt{N}$. Making the substitutions $u' = \sqrt{N}u$ and $w' = \sqrt{N}w$, the double integral is now

$$\begin{aligned}
&\frac{1}{(2\pi i)^2} \oint_{|u|=1/\sqrt{N}} \oint_{|w|=2/\sqrt{N}} \frac{e^{\gamma^+ u^{-1}+\gamma^- u}}{e^{\gamma^+ w^{-1}+\gamma^- w}} \frac{u^{x_i} e^{n_i \ln(1-u)}}{w^{x_j+1} e^{n_j \ln(1-w)}} \frac{du\,dw}{w-u} N^{(x_i-x_j)/2}\bigl(\gamma^+\bigr)^{(x_j-x_i)/2} \\
&\quad= \frac{1}{(2\pi i)^2} \oint_{|u'|=1} \oint_{|w'|=2} \frac{e^{\gamma^+ u'^{-1}\sqrt{N}+\gamma^- u'/\sqrt{N}}}{e^{\gamma^+ w'^{-1}\sqrt{N}+\gamma^- w'/\sqrt{N}}} \frac{u'^{x_i} e^{n_i \ln(1-u'/\sqrt{N})}}{w'^{x_j+1} e^{n_j \ln(1-w'/\sqrt{N})}} \frac{du'\,dw'}{w'-u'} \bigl(\gamma^+\bigr)^{(x_j-x_i)/2} \\
&\quad= \frac{1}{(2\pi i)^2} \oint_{|u'|=1} \oint_{|w'|=2} \frac{e^{\sqrt{N}(\gamma^+ u'^{-1}+c\log u'-u'+O(1/\sqrt{N}))}}{e^{\sqrt{N}(\gamma^+ w'^{-1}+c\log w'-w'+O(1/\sqrt{N}))}} \frac{du'\,dw'}{w'(w'-u')} \bigl(\gamma^+\bigr)^{(x_j-x_i)/2}.
\end{aligned}$$

In general $|e^z| = e^{\Re z}$, so consider the real part of the function in the exponent, $A(z) = \gamma^+ z^{-1} + c\log z - z$. Note that $A'(z) = 0$ at $z_+ = \frac{c}{2} + \frac{\sqrt{c^2-4\gamma^+}}{2}$ and $z_- = \bar{z_+}$.

The basic idea of the rest of the proof can be summarized as follows. The term $\sqrt{\gamma^+}^{x_j-x_i}$ creates a $e^{\sqrt{N}(-c\log\sqrt{\gamma^+})}$ term in both the numerator and denominator. So it is equivalent to analyze $\Re(A(z) - c\log\sqrt{\gamma^+}) = \Re(A(z) - A(z_+))$. We deform the u and w contours in such a way that $\Re(A(u) - A(z_+)) < 0$ and $\Re(A(w) - A(z_+)) > 0$, which will cause the integrand to converge to 0 as $N \to \infty$. However, the deformation of the contours causes the integral to pick up residues at $u = w$. These residues occur on a circular arc from z_- to z_+. If $c = 2\sqrt{\gamma^+}$, then $z_+ = z_- > 0$, so the arc consists of a single point. As c decreases, z_+ moves counterclockwise around the circle $|z| = \sqrt{\gamma^+}$ while z_- moves clockwise. This means that the arc becomes increasingly large as c decreases from $2\sqrt{\gamma^+}$ to $-2\sqrt{\gamma^+}$. When $c = -2\sqrt{\gamma^+}$, then $z_+ = z_- < 0$, so the arc has becomes the whole circle around the origin.

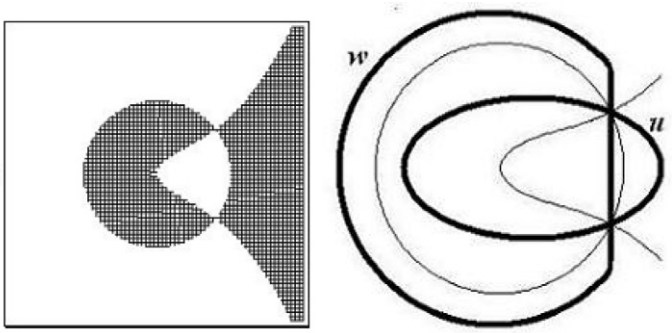

Fig. 6. On the left is $\Re(A(z) - c\log\sqrt{\gamma^+})$, where the black regions indicate $\Re < 0$ and the white regions indicate $\Re > 0$. The u-contour is contained in the black regions, while the w contour is contained in the white regions.

We then need to consider

$$-\frac{1}{2\pi i}\oint_{|z|=r<1}\frac{z^{x_i-x_j-1}}{(1-z)^{n_j-n_i}}\,dz,$$

which occurs when $n_i < n_j$. The expression for the residue at $u = w$ has the same integrand. With the minus sign, the integration contour for z goes clockwise along a circle around the origin. Therefore it will cancel the circular arc from z_- to z_+. This explains why the integration contour in S_{z_+} crosses $(0,\infty)$ when $t_i \geqslant t_j$ and $(-\infty, 0)$ when $t_i < t_j$.

Case 1: $-2\sqrt{\gamma^+} < c < 2\sqrt{\gamma^+}$. Observe that $\Re(A(z) - A(z_+)) = 0$ for all $|z| = |z_\pm| = |\sqrt{\gamma^+}|$. Also notice that $A(z) - A(z_+)$ has a double zero at z_+ and z_-. See Fig. 6.

If the contours of integration are deformed as shown in Fig. 6, then

$$\frac{e^{\sqrt{N}(\gamma^+u'^{-1}+c\log u'-u'+O(1/\sqrt{N}))}}{e^{\sqrt{N}(\gamma^+w'^{-1}+c\log w'-w'+O(1/\sqrt{N}))}}\to 0$$

as $N\to\infty$. The integral thus approaches zero, except for the residues at $u = w$. So $\sqrt{N}^{x_i-x_j}K(n_i,x_i;n_j,x_j)$ converges to

$$\sqrt{N}^{x_i-x_j}\frac{1}{2\pi i}\int_{z_-/\sqrt{N}}^{z_+/\sqrt{N}}\frac{du}{u^{x_j-x_i+1}}(1-u)^{n_i-n_j}\to\frac{1}{2\pi i}\int_{z_-}^{z_+}u^{x_i-x_j-1}e^{-(t_i-t_j)u}\,du.$$

If $t_i \geqslant t_j$, then the integration contour crosses $(0,\infty)$. If $t_i < t_j$, then the contour crosses $(-\infty, 0)$.

Case 2: $c^2 - 4\gamma^+ > 0$ and $c > 0$. Deforming the contours of integration as shown in Fig. 7, the integral becomes zero. The contours do not pass through each other, so no residues appear. So $\sqrt{N}^{x_i-x_j}K(n_i,x_i;n_j,x_j)\to 0$ if $t_i \geqslant t_j$. This means that $\det[K(n_i,x_i;n_j,x_j)]\to 0$.

Case 3: $c^2 - 4\gamma^+ > 0$ and $c < 0$. Deform the contours as shown in Fig. 8. Since the w and u contours pass through each other during the deformation, the integral picks up residues at $u = w$. So if $t_i \geqslant t_j$, then $\sqrt{N}^{x_i-x_j}K(n_i,x_i;n_j,x_j)$ converges to

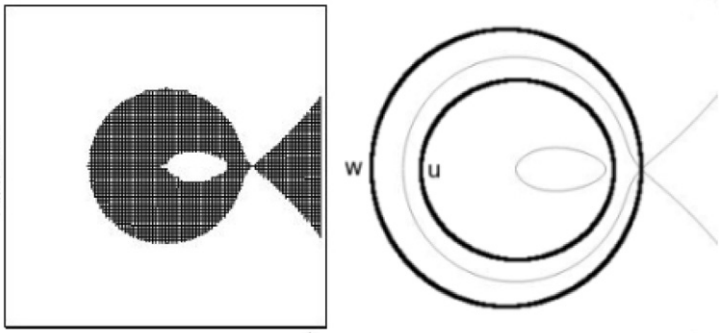

Fig. 7. Again, the figure on the left shows $\Re(A(z) - A(z_+))$, with black regions indicating $\Re < 0$ and white regions indicating $\Re > 0$.

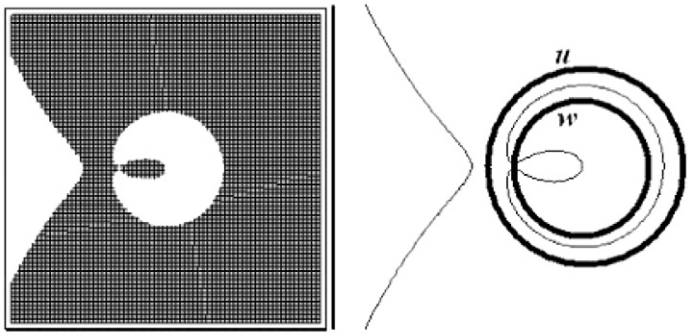

Fig. 8. On the left is $\Re(A(z) - c \log \sqrt{\gamma^+})$, where the black regions indicate $\Re < 0$ and the white regions indicate $\Re > 0$.

$$\sqrt{N}^{x_i - x_j} \frac{1}{2\pi i} \oint w^{x_i - x_j - 1} (1-w)^{n_i - n_j} \, dw = \frac{1}{2\pi i} \oint w^{x_i - x_j - 1} e^{(t_j - t_i)w} \, dw$$
$$= \frac{(t_j - t_i)^{x_j - x_i}}{(x_j - x_i)!}$$

If $t_i < t_j$, then there is the integral in z, which cancels with the residues at $u = w$, so $\sqrt{N}^{x_i - x_j} K(n_i, x_i; n_j, x_j)$ converges to 0. This means that the matrix $[K(n_i, x_i; n_j, x_j)]$ asymptotically has ones on the diagonal and zeroes below. So $\det[K(n_i, x_i; n_j, x_j)]$ converges to 1. □

Remark. It is natural to ask what happens when $x_i/\sqrt{N}$ do not all converge to the same real number. If $x_i/\sqrt{N}$ and $x_j/\sqrt{N}$ converge to different real numbers, then $x_i - x_j$ diverges. In that case, $K(n_i, x_i; n_j, x_j) \to 0$. So the determinant $\det[K(n_i, x_i; n_j, x_j)]$ factors into blocks corresponding to distinct values of $\lim x_i/\sqrt{N}$. Probabilistically, this means that the probability of finding a vertical edge becomes independent in different parts of the boundary.

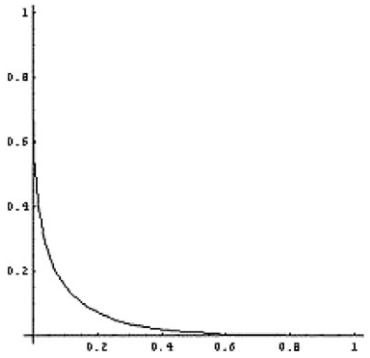

Fig. 9. This figure shows the equations in (9), with a plotted on the horizontal axis and b plotted on the vertical with parameter z_0.

4.4. Bulk limits with $\gamma^{\pm} \propto N$

We now let $\gamma^{\pm}$ depend on N in such a way that $\gamma^{+}/N \to a > 0$ and $\gamma^{-}/N \to b > 0$ as $N \to \infty$. Before we can state the result, some preliminary definitions and lemmas are needed.

For $a, b > 0$ and $c \in \mathbb{R}$, recall that

$$R_{a,b,c}(z) = -bz^3 + (b - c - 1)z^2 + (c + a)z - a.$$

Lemma 4.4.

(1) *The cubic polynomial $R_{a,b,c}(z)$ has a multiple root iff c is a root of $Q_{a,b}(z)$, where $Q_{a,b}(z)$ is defined in Section* 3.1.
(2) *Let $q_1 \leqslant \cdots \leqslant q_m$ be the real roots of $Q_{a,b}$. If $q_1 < c < q_2$ or $q_{m-1} < c < q_m$ then $R_{a,b,c}(z)$ has a pair of complex conjugate roots.*

Proof. (1) In general, a polynomial has a multiple root iff its discriminant is zero. The discriminant of $R_{a,b,c}$ is exactly $Q_{a,b}(c)/16$.

(2) A cubic polynomial has nonreal roots iff its discriminant is negative. Since $Q_{a,b}$ diverges to $+\infty$ in both directions, $Q_{a,b}(z)$ is negative for $q_1 < z < q_2$ and $q_{m-1} < z < q_m$. □

Lemma 4.5. *The polynomial $Q_{a,b}$ has a double root at c_0 iff a, b and c_0 satisfy the equations*

$$a = \frac{z_0^3}{(z_0 - 1)^3}, \qquad b = -\frac{1}{(z_0 - 1)^3}, \qquad c_0 = -\frac{z_0^2(z_0 - 3)}{(z_0 - 1)^3} \tag{9}$$

for some $z_0 \in \mathbb{R}$.

Proof. Since $Q_{a,b}(c_0)$ is the discriminant of R_{a,b,c_0}, $Q_{a,b}(z)$ has a double root at c_0 iff $R_{a,b,c_0}(z)$ has a triple root. For any z_0, R has a triple root at z_0 iff $R(z_0) = R'(z_0) = R''(z_0) = 0$. This gives three linear equations in the three variables a, b, and c_0, which can be solved explicitly. □

Remark. We have $a, b > 0$ iff $z_0 < 0$. Then $-1 < c_0 < 0$. See Fig. 9.

One more definition is needed before we can state the main result of this section. Let B be the incomplete beta kernel defined by

$$\mathrm{B}(k,l;z)=\frac{1}{2\pi i}\int_{\bar{z}}^{z}(1-u)^k u^{-l-1}\,du,$$

where the path of integration crosses $(0,1)$ for $k\geqslant 0$ and $(-\infty,0)$ for $k<0$. The incomplete beta kernel has been introduced in [27]. It is one of the extensions of the discrete sine kernel of [5].

Theorem 4.6. *Let $\gamma^+/N\to a$ and $\gamma^-/N\to b$ for positive real numbers a and b. Also let $x_1,\dots,x_k$ and $n_1,\dots,n_k$ depend on N in such a way that n_i-n_j and are x_i-x_j constant, $n_j/N\to 1$ and $x_j/N\to c$ for all $1\leqslant i,j\leqslant k$. Let $q_1\leqslant\cdots\leqslant q_m$ denote the distinct real roots of $Q_{a,b}(x)$ (m can be 2, 3, or 4). Additionally, assume $Q_{a,b}(c)\neq 0$. Let z_+ be a root of $R_{a,b,c}(x)$ such that $\Im(z_+)\geqslant 0$ (cf. Lemma 4.4). If $m=4$, then*

$$\det\big[K(n_i,x_i;n_j,x_j)\big]_{1\leqslant i,j\leqslant k}\to\begin{cases}0, & c\leqslant q_1,\\ \det[\mathrm{B}(n_i-n_j,x_j-x_i;z_+)]_{1\leqslant i,j\leqslant k}, & q_1<c<q_2,\\ 1, & q_2\leqslant c\leqslant q_3,\\ \det[\mathrm{B}(n_i-n_j,x_j-x_i;z_+)]_{1\leqslant i,j\leqslant k}, & q_3<c<q_4,\\ 0, & c\geqslant q_4.\end{cases}$$

If $m=2$ or 3, then

$$\det\big[K(n_i,x_i;n_j,x_j)\big]_{1\leqslant i,j\leqslant k}\to\begin{cases}0, & c\leqslant q_1,\\ \det[\mathrm{B}(n_i-n_j,x_j-x_i;z_+)]_{1\leqslant i,j\leqslant k}, & q_1<c<q_m,\\ 0, & c\geqslant q_m.\end{cases}$$

Proof. The double integral in the correlation kernel of Theorem 3.1 asymptotically becomes

$$\left(\frac{1}{2\pi i}\right)^2\oint\oint\frac{e^{N(au^{-1}+bu+c\log(u)+\log(1-u)+O(1/N))}}{e^{N(aw^{-1}+bw+c\log(u)+\log(1-u)+O(1/N))}}\,\frac{du\,dw}{w(u-w)}$$

where the contours are over $|u|=r$ and $|w-1|=\epsilon<1-r$. So we can perform a similar analysis as in Theorem 4.2, except with a more complicated $A(z)=az^{-1}+bz+c\log(z)+\log(1-z)$. For this proof, it is actually more convenient to write $A(z;c)$ in place of $A(z)$.

First we find which values of c correspond to the edges of the hypothetical limit shape in Fig. 4. These are the values of c such that $A(z;c)-A(z_0;c)$ has a triple zero for some $z_0\in\mathbb{C}$. Requiring $A(z;c)-A(z_0;c)$ to have a triple zero at $z=z_0$ is equivalent to requiring $A'(z;c)$ to have a double zero at $z=z_0$. Multiplying the equation $A'(z;c)=0$ by $z^2(1-z)$ gives the equation $R_{a,b,c}(z)=0$ (note that $R_{a,b,c}(0)=-a$ and $R_{a,b,c}(1)=-1$, which are both nonzero). By Lemma 4.4, $R_{a,b,c}$ has a double zero iff $c=q_1,\dots,q_m$.

Now we need to determine how to deform the contours appropriately. The analysis here is almost identical to that of Theorem 4.2. We want to find nonreal values of z_0 such that $A(z;c)-A(z_0;c)$ has a double zero. This reduces to looking for nonreal roots of $R_{a,b,c}(z)$

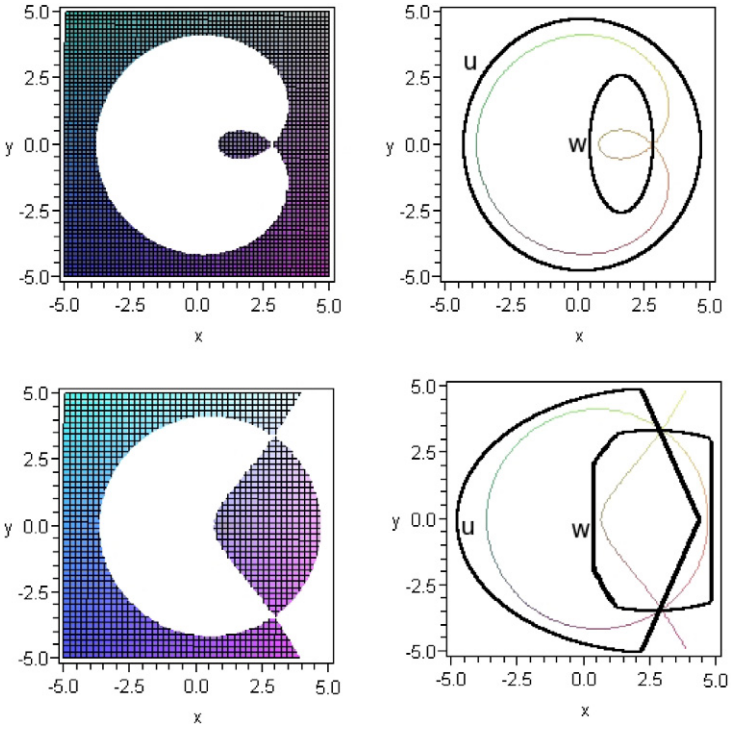

Fig. 10. The shaded regions show $\Re(A(z;c) - A(z_+;c)) < 0$, while the white regions show $\Re > 0$. The first row corresponds to $c < q_1$, the second row corresponds to $q_1 < c < q_2$, the third corresponds to $q_2 < c < q_3$, the fourth corresponds to $q_3 < c < q_4$, and the fifth corresponds to $c > q_4$.

in the upper half-plane, which we have defined to be z_+. As can be seen from Fig. 4, there are potentially five different regions of behavior for the bulk limits. The corresponding behavior of $\Re(A(z;c) - A(z_+;c))$ is shown in Fig. 10. (These are computer generated figures for specific values of parameters, however, it is not hard to prove that similar figures arise for any values of the parameters in the corresponding domains. An example of such an argument can be found in the beginning of the proof of Theorem 4.9 below.) The arguments of Theorem 4.2 are again applicable here, except with the new definition of z_+. □

4.5. The Airy kernel as an edge limit

Before stating the main result, some definitions are needed.

Let $Ai(x)$ denote the Airy function:

$$Ai(x) = \frac{1}{2\pi} \int_{-\infty}^{\infty} e^{is^3/3 + ixs}\, ds.$$

This integral only converges conditionally. Shift the contour of integration as shown in Fig. 11. Along this contour, the function $e^{is^3/3}$ is real and decreases superexponentially.

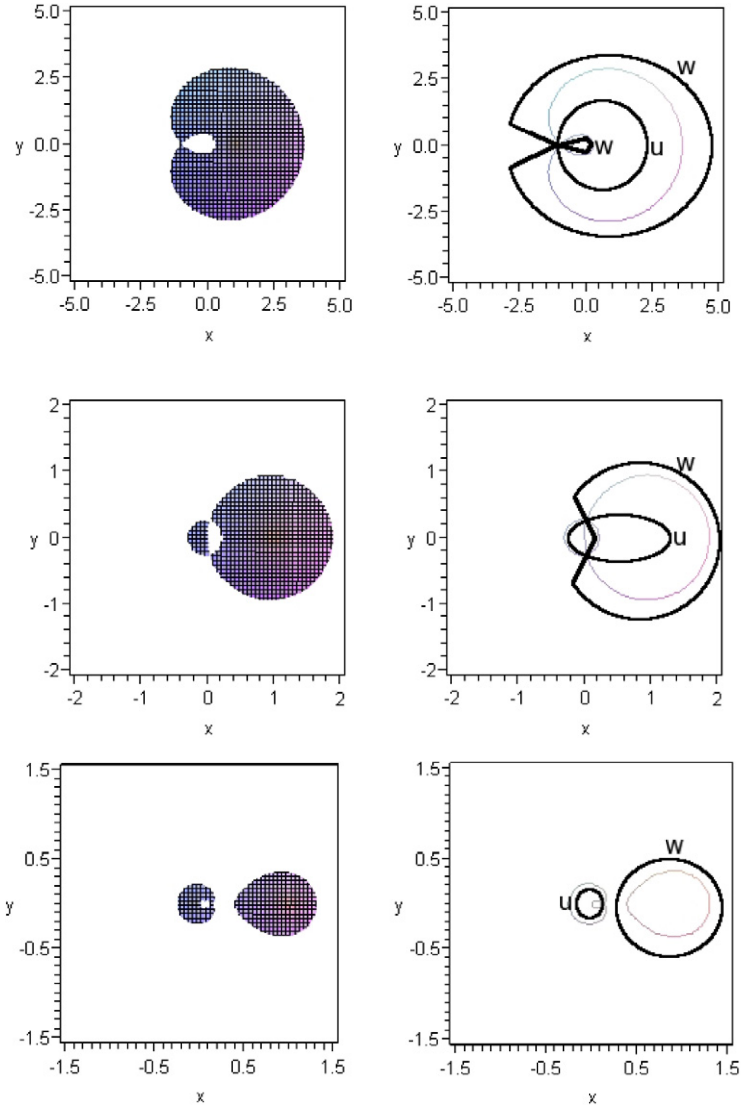

Fig. 10. (*continued*)

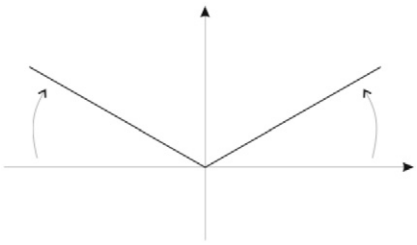

Fig. 11. A better contour for the Airy function. The contour goes from $\infty e^{5\pi i/6}$ to 0 to $e^{\pi i/6}$.

Define the *extended Airy kernel* $\mathcal{A}$ to be

$$\mathcal{A}(\tau_1,\sigma_1;\tau_2,\sigma_2)=\begin{cases}\int_0^\infty e^{-\lambda(\tau_1-\tau_2)}Ai(\sigma_1+\lambda)Ai(\sigma_2+\lambda)\,d\lambda & \text{if } \tau_1\geqslant\tau_2,\\ -\int_{-\infty}^0 e^{-\lambda(\tau_1-\tau_2)}Ai(\sigma_1+\lambda)Ai(\sigma_2+\lambda)\,d\lambda & \text{if } \tau_1<\tau_2.\end{cases}\tag{10}$$

It was first obtained in [30] in the context of the polynuclear growth model.

There is a useful representation for $\mathcal{A}$ as a double integral.

Proposition 4.7. *(See [19, §2.2].) Let ν_1,ν_2 satisfy $\nu_1+\nu_2+\tau_1-\tau_2>0$. If $\tau_1\geqslant\tau_2$, then*

$$\mathcal{A}(\tau_1,\sigma_1;\tau_2,\sigma_2)=\left(\frac{1}{2\pi i}\right)^2\int_{\Im(u)=\nu_1}\int_{\Im(w)=\nu_2}\frac{e^{i\sigma_1u+i\sigma_2w+i(w^3+u^3)/3}}{\tau_2-\tau_1+i(w+u)}\,du\,dw.$$

If $\tau_1<\tau_2$, then

$$\begin{aligned}&\mathcal{A}(\tau_1,\sigma_1;\tau_2,\sigma_2)\\&\quad=\left(\frac{1}{2\pi i}\right)^2\int_{\Im(u)=\nu_1}\int_{\Im(w)=\nu_2}\frac{e^{i\sigma_1u+i\sigma_2w+i(w^3+u^3)/3}}{\tau_2-\tau_1+i(w+u)}\,du\,dw\\&\qquad-\frac{1}{\sqrt{4\pi(\tau_2-\tau_1)}}\exp\left(-\frac{(\sigma_1-\sigma_2)^2}{4(\tau_2-\tau_1)}-\frac{1}{2}(\tau_2-\tau_1)(\sigma_1+\sigma_2)+\frac{1}{12}(\tau_2-\tau_1)^3\right).\end{aligned}$$

The double integral from Proposition 4.7 can be rewritten as

$$\begin{aligned}&\left(\frac{1}{2\pi i}\right)^2\iint\exp\Big(\tau_1\sigma_1-\tau_2\sigma_2-\frac{1}{3}\tau_1^3+\frac{1}{3}\tau_2^3-\big(\sigma_1-\tau_1^2\big)u+\big(\sigma_2-\tau_2^2\big)w\\&\qquad-\tau_1u^2+\tau_2w^2+\frac{1}{3}\big(u^3-w^3\big)\Big)\frac{du\,dw}{u-w}.\end{aligned}\tag{11}$$

Indeed, just as we deformed the contours of integration for $Ai(x)$, we can deform the contours of integration in Proposition 4.7. The u-contour can be taken over $i\nu_1+\infty e^{5\pi i/6}$ to $i\nu_1$ to $i\nu_1+e^{\pi i/6}$, while the w-contour can be taken from $i\nu_2+\infty e^{5\pi i/6}$ to $i\nu_2$ to $i\nu_2+e^{\pi i/6}$. Integrating along these contours also allows for the possibility of $\nu_1+\nu_2+\tau_1-\tau_2=0$. If we further make the substitutions $w=-iw'+\nu_2 i$ and $u=iu'+\nu_1 i$, then the double integral becomes

$$\begin{aligned}&\left(\frac{1}{2\pi i}\right)^2\iint\exp\Big(-\nu_1\sigma_1-\nu_2\sigma_2+\frac{1}{3}\nu_1^3+\frac{1}{3}\nu_2^3-\big(\sigma_1-\nu_1^2\big)u+\big(\sigma_2-\nu_2^2\big)w\\&\qquad+\nu_1u^2+\nu_2w^2+\frac{1}{3}\big(u^3-w^3\big)\Big)\frac{du\,dw}{-\tau_2+\tau_1+\nu_1+\nu_2+u-w},\end{aligned}$$

where u is integrated from $\infty e^{-\pi i/3}$ to 0 to $\infty e^{\pi i/3}$ and w is integrated from $\infty e^{4\pi i/3}$ to 0 to $\infty e^{2\pi i/3}$. Taking $\nu_1=-\tau_1$ and $\nu_2=\tau_2$ turns the double integral into (11). Writing the double integral in this form is useful when proving the following result.

In the next statement, let $Q_{a,b}$ be the same polynomial as in Section 3.1, see also Section 3.4.

Theorem 4.8. *Let $\gamma^+/N \to a, \gamma^-/N \to b$ for positive real numbers a and b. Let c_1 be a root of $Q_{a,b}(z)$ and z_1 be the double zero of $R_{a,b,c_1}(z)$. Let $n_1, \dots, n_k$ depend on N in such a way that*

$$\frac{n_j - N}{N^{2/3}} \to t_j \in \mathbb{R} \quad \text{as } N \to \infty.$$

Let $\tilde{t}_j = t_j z_1 (1 - z_1)^{-1}$ and let $x_1, \dots, x_k$ depend on N in such a way that

$$\frac{x_j - c_1 N - \tilde{t}_j N^{2/3}}{N^{1/3}} \to s_j \in \mathbb{R} \quad \text{as } N \to \infty.$$

If $c_1 > 0$ or $c_1 < -1$, set $\mathcal{K} = K$. Otherwise, set $\mathcal{K} = K_\Delta$. Then as $N \to \infty$,

$$\det\left[\left|z_1 p_3^{1/3}\right| N^{1/3} \mathcal{K}(n_i, x_i; n_j, x_j)\right]_{1 \leqslant i,j \leqslant k} \to \det\left[\mathcal{A}(\tau_i, \sigma_i; \tau_j, \sigma_j)\right]_{1 \leqslant i,j \leqslant k}.$$

Here, p_3 denotes the constant

$$-\frac{1}{(1 - z_1)^3} - \frac{3a}{z_1^4} + \frac{c_1}{z_1^3}$$

and

$$\tau_m = \frac{t_m}{2(p_3)^{2/3}(z_1 - 1)^2 z_1}, \qquad \sigma_m = \tau_m^2 - \frac{s_m}{z_1 p_3^{1/3}}, \quad 1 \leqslant m \leqslant k.$$

Remark. The statement may seem a bit cryptic. Let us explain it in words. There are (potentially) four edge points (points where the curve becomes horizontal or vertical) as seen in the top curve in Fig. 4. We consider K for the first point (when $c_1 > 0$) and the fourth point (when $c_1 < -1$), which means that we look at the largest rows of λ^+ and λ^-. For the second and third points we consider K_Δ, which means that we look at the largest columns of λ^+ and λ^-. For the second and fourth points, $\det[z_1 p_3^{1/3} \mathcal{K}] \to \det[\mathcal{A}]$, while for the first and third points $\det[-z_1 p_3^{1/3} \mathcal{K}] \to \det[\mathcal{A}]$. At the second and fourth points $z_1 p_3^{1/3}$ is positive, while at the first and third points $z_1 p_3^{1/3}$ is negative. This corresponds to the fact that in order to obtain the Airy process we need to flip the sign of particles at the lower edges of λ^+ and λ^- (the second and fourth edge points, respectively).

Proof. This proof is similar to the proof of Theorem 4.9, so some of the details will be omitted.

Once again, let $A(z; c; d)$ denote $az^{-1} + bz + c \log z + d \log(1 - z)$. Multiplying by the conjugating factor

$$\frac{e^{-NA(z_1; x_i/N; n_i/N)}}{e^{-NA(z_1; x_j/N; n_j/N)}} = \frac{z_1^{-x_i}}{z_1^{-x_j}} \frac{(1 - z_1)^{-n_i}}{(1 - z_1)^{-n_j}} \frac{e^{-aNz_1^{-1}}}{e^{-aNz_1^{-1}}} \frac{e^{-bNz_1}}{e^{-bNz_1}}$$

allows us to consider $A(z; x_m/N; n_m/N) - A(z_1; x_m/N; n_m/N)$ instead of $A(z; x_m/N; n_m/N)$. The Taylor expansion yields

$$N\left(A\left(z; c_1 + \frac{\tilde{t}_m}{N^{1/3}} + \frac{u_m}{N^{2/3}}; 1 + \frac{t_m}{N^{1/3}}\right) - A\left(z_1; c_1 + \frac{\tilde{t}_m}{N^{1/3}} + \frac{u_m}{N^{2/3}}; 1 + \frac{t_m}{N^{1/3}}\right)\right)$$
$$= \frac{1}{3}(z')^3 - \frac{t_m}{2(p_3)^{2/3}(z_1-1)^2 z_1}(z')^2 + \frac{s_m}{(p_3)^{1/3} z_1} z' + o(1)$$

where $z' = (p_3)^{1/3} N^{1/3}(z - z_1)$. The contours of integration for u and w are shown in Fig. 12. Now let $u' = (p_3)^{1/3} N^{1/3}(u - z_1)$ and $w' = (p_3)^{1/3} N^{1/3}(w - z_1)$. Just like in the proof of Theorem 4.9, the Taylor series gives rise to the exponential terms in 11. In addition, the term $\frac{du\,dw}{u-w}$ becomes $N^{-1/3} p_3^{-1/3}$, while the extra w in the denominator becomes z_1^{-1}. We break down the following analysis into cases.

Case 1: $c_1 > 0$. This corresponds to the fourth row in Fig. 12 and the top edge point of Fig. 3. In this case, p_3 is negative, so the contours for u' and w' agree with the contours in expression (11). Since $0 < z_1 < 1$, this implies that $\tilde{t}_j - \tilde{t}_i > 0$ if $t_j - t_i > 0$. Since $n_j > n_i$ translates to $t_j > t_i$, this means that $x_j - x_i$ can be assumed positive if $n_j > n_i$. Therefore the integral in z from expression (4) can be written as

$$-\binom{n_j - n_j + x_j - x_i - 1}{x_j - x_i} = -\binom{n_j - n_i + x_j - x_i}{x_j - x_i} \frac{n_j - n_i}{n_j - n_i + x_j - x_i}.$$

Using the Laplace–Demoivre Theorem shows that

$$-N^{1/3} \frac{z_1^{x_j - x_1}}{(1-z_1)^{n_i - n_j}} \binom{n_j - n_i + x_j - x_i - 1}{x_j - x_i}$$
$$\to -\frac{|1 - z_1|}{\sqrt{2\pi |z_1| (t_j - t_i)}} \exp\left(-\frac{(1-z_1)^2}{2|z_1|} \frac{(s_j - s_i)^2}{|t_j - t_i|}\right). \tag{12}$$

Taking the last term in Proposition 4.7 and multiplying by $\exp(-\tau_1\sigma_1 + \tau_2\sigma_2 + \frac{1}{3}\tau_1^3 - \frac{1}{3}\tau_2^3)$ yields

$$-|p_3|^{1/3} |z_1|^{1/2} \frac{|1 - z_1|}{\sqrt{2\pi (t_j - t_i)}} \exp\left(-\frac{(1-z_1)^2}{2z_1} \frac{(s_j - s_i)^2}{t_j - t_i}\right).$$

We have seen that

$$\left|z_1 p_3^{1/3}\right| N^{1/3} \frac{z_1^{x_j - x_1}}{(1-z_1)^{n_i - n_j}} K(n_i, x_i; n_j, x_j)$$
$$\to \exp\left(-\tau_1\sigma_1 + \tau_2\sigma_2 + \frac{1}{3}\tau_1^3 - \frac{1}{3}\tau_2^3\right) \mathcal{A}(\tau_i, \sigma_i; \tau_j, \sigma_j), \tag{13}$$

which gives the result.

Case 2: $c_1 < -1$. This corresponds to the first row in Fig. 12. Here, $z_1 > 1$ and $p_3 > 0$. Making the deformations gives residues at $u = w$, which can be written as

$$-\frac{1}{2\pi i} \oint_{|z-1| = \epsilon < 1} \frac{z^{x_i - x_j - 1}}{(1-z)^{n_j - n_i}}\, dz.$$

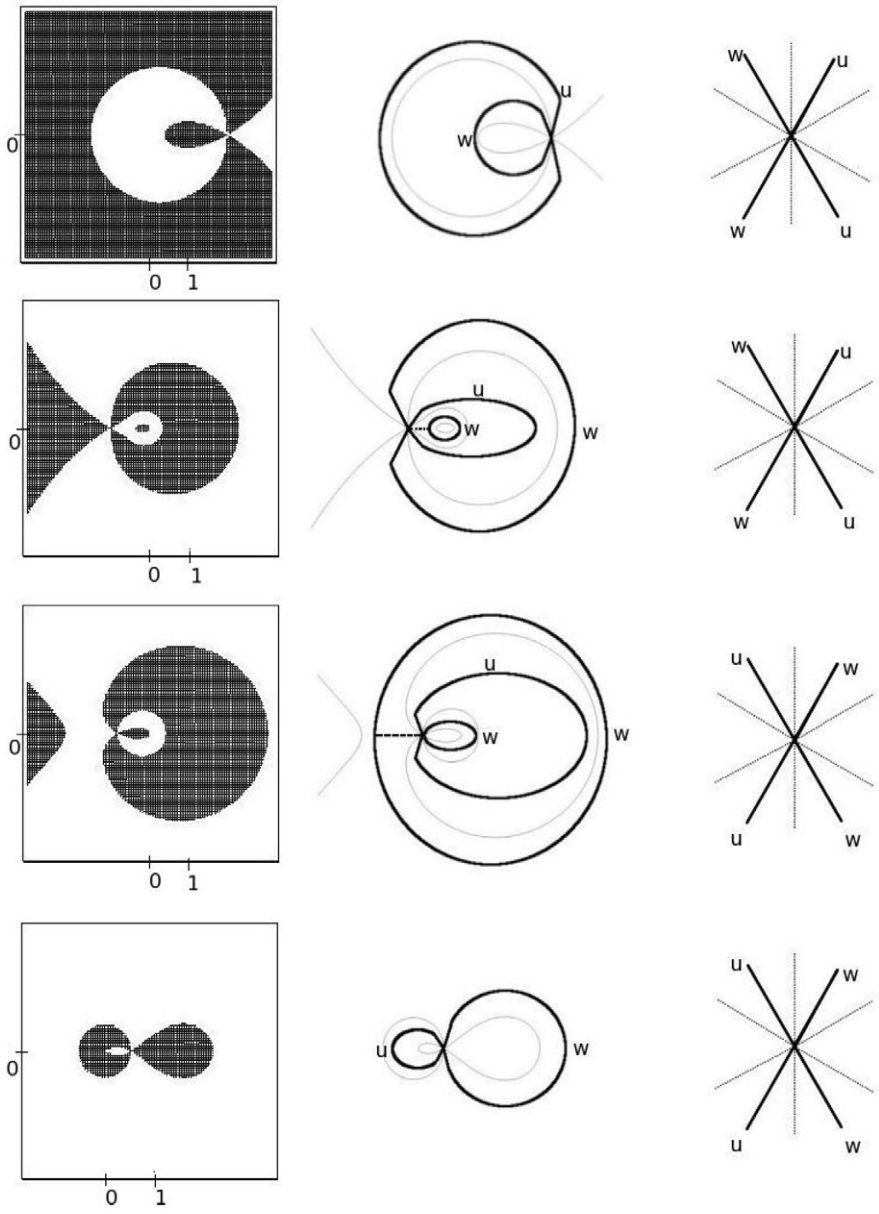

Fig. 12. The left column shows $\Re(A(z; c_0; 1) - A(z_0; c_0; 1))$, with shaded regions showing $\Re < 0$ and white regions showing $\Re > 0$. The right column shows the local behavior around z_1. The first row occurs when c_1 is the smallest real root of $Q_{a,b}$, the second row when c_1 is the second smallest real root, and so forth. If $Q_{a,b}$ has only two real roots, the middle two rows do not occur.

If $n_i \geqslant n_j$, then these residues are zero. If $n_i < n_j$, then $t_i < t_j$, which implies $x_i > x_j$, so the integral in z from expression (4) is zero. So when $n_i < n_j$, the extra term can be written as

$$(-1)^{n_j-n_i-1}\binom{x_i-x_j-1}{n_j-n_i-1}=(-1)^{n_j-n_i-1}\binom{x_i-x_j}{n_j-n_i}\frac{n_j-n_i}{x_i-x_j}.$$

Using Laplace–Demoivre, this binomial converges to the right-hand side of Eq. 12. So expression (13) holds.

Case 3: $-1<c_1<0$. If a and b are small enough, then $Q_{a,b}$ has two roots between -1 and 0. The second row in Fig. 12 corresponds to the smaller root, while the third row corresponds to the larger root. In the second row p_3 is positive, while in the third row p_3 is negative. In both rows $z_1<0$.

Making the deformations gives residues at $u=w$, which can be written as

$$-\frac{1}{2\pi i}\oint_{|z|=r<1}\frac{z^{x_i-x_j-1}}{(1-z)^{n_j-n_i}}\,dz.$$

If $n_i\leqslant n_j$, then this expression cancels with the z-integral in expression (5). If $n_i>n_j$, then the extra term can be written as

$$-(-1)^{x_j-x_i}\binom{n_i-n_j}{x_j-x_i}.$$

Once again, this converges to expression (12). So expression (13) holds. □

4.6. The Pearcey kernel as an edge limit

We now find the edge limit at the point where the two limit curves in the middle figure in Fig. 4 just barely merge. In this case, we analyze the limiting behavior of K_Δ from Corollary 3.2 instead of K, which corresponds to the fact that we consider the limit of the point process formed by columns of $\lambda^{\pm}$ rather than by their rows, see Fig. 1.

Theorem 4.9. *Fix $z_0<0$ and let a, b and c_0 satisfy Eqs.* (9). *Let $\gamma^+/N\to a$ and $\gamma^-/N\to b$ as $N\to\infty$. Let $n_1,\dots,n_k$ depend on N in such a way that $(n_j-N)/\sqrt{N}\to 2t_j\in\mathbb{R}$ as $N\to\infty$. Set $\zeta=(z_0-1)|z_0|^{-1/2}<0$. Define*

$$\tilde{t}_j=\frac{z_0}{1-z_0}t_j$$

and let $x_1,\dots,x_k$ depend on N in such a way that

$$\frac{\zeta(x_j-c_0N-\tilde{t}_j\sqrt{N})}{N^{1/4}}\to s_j\in\mathbb{R}$$

as $N\to\infty$. Then as $N\to\infty$,

$$\det\big[-\zeta^{-1}N^{1/4}K_\Delta(n_i,x_i;n_j,x_j)\big]_{1\leqslant i,j\leqslant k}\to\det\big[P(t_i,s_i;t_j,s_j)\big]_{1\leqslant i,j\leqslant k}$$

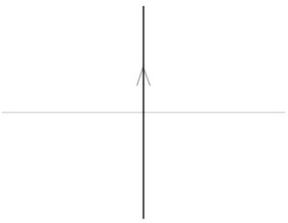

Fig. 13. The contour for u.

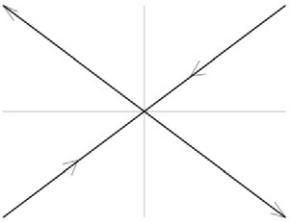

Fig. 14. The contour for w.

where

$$P(t_i,s_i;t_j,s_j)=\left(\frac{1}{2\pi i}\right)^2\iint e^{w^4-u^4+t_iu^2-t_jw^2+s_iu-s_jw}\,\frac{du\,dw}{u-w}$$
$$-\frac{1}{\sqrt{2\pi|t_i-t_j|}}\exp\left(-\frac{(s_j-s_i)^2}{2(t_i-t_j)}\right),\quad t_i>t_j,$$
$$\left(\frac{1}{2\pi i}\right)^2\iint e^{w^4-u^4+t_iu^2-t_jw^2+s_iu-s_jw}\,\frac{du\,dw}{u-w},\quad t_i\leqslant t_j, \tag{14}$$

where u is integrated from $-i\infty$ to $i\infty$ and w is integrated on the rays from $\pm\infty e^{i\pi/4}$ to 0 to $\pm\infty e^{-i\pi/4}$ as in Figs. 13 *and* 14.

The kernel $P(t_i,s_i;t_j,s_j)$ is called the Pearcey kernel and it was previously obtained in [1, 13,14,28,31].

Proof. The argument is similar to the proofs of Theorems 4.2 and 4.6. It is convenient to let $A(z;c;d)$ denote $az^{-1}+bz+c\log z+d\log(1-z)$. Then the double integral in the correlation kernel of Corollary 3.2 becomes asymptotically

$$-\left(\frac{1}{2\pi i}\right)^2\iint\frac{e^{N(au^{-1}+bu+(x_i/N)\log u+(n_i/N)\log(1-u)+O(1/N))}}{e^{N(aw^{-1}+bw+(x_j/N)\log w+(n_j/N)\log(1-w)+O(1/N))}}\,\frac{du\,dw}{w(u-w)} \tag{15}$$
$$=-\left(\frac{1}{2\pi i}\right)^2\iint\frac{e^{N(A(u;x_i/N;n_i/N)+O(1/N))}}{e^{N(A(w;x_j/N;n_j/N)+O(1/N))}}\,\frac{du\,dw}{w(u-w)}. \tag{16}$$

Multiplying the integrand by the conjugating factor

$$\frac{e^{-NA(z_0;x_i/N;n_i/N)}}{e^{-NA(z_0;x_j/N;n_j/N)}}=\frac{z_0^{-x_i}}{z_0^{-x_j}}\,\frac{(1-z_0)^{-n_i}}{(1-z_0)^{-n_j}}\,\frac{e^{-aNz_0^{-1}}}{e^{-aNz_0^{-1}}}\,\frac{e^{-bNz_0}}{e^{-bNz_0}},$$

which cancels when taking the determinant for correlation functions, allows us to consider $A(z;x_m/N;n_m/N)-A(z_0;x_m/N;n_m/N)$ instead of $A(z;x_m/N;n_m/N)$.

Deform the contours as shown in Fig. 15. Let us show that these contours exist. We know that the level lines only intersect at z_0 (the only critical point of the function $A(z;c_0;1)-A(z_0;c_0;1)$, since $A'(z)=-b(z-z_0)^3z^{-2}(1-z)^{-1}$), and they are symmetric with respect to the real axis.

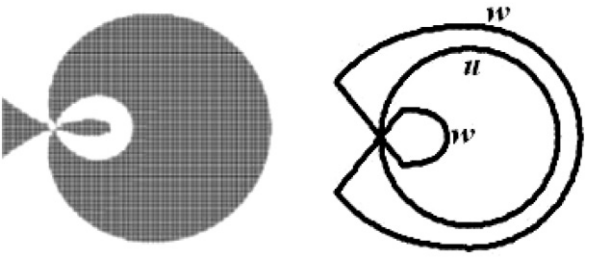

Fig. 15. The figure on the left shows $\Re(A(z; c_0; 1) - A(z_0; c_0; 1))$, with black regions indicating $\Re < 0$ and white regions indicating $\Re > 0$.

Restrict $\Re(A(z; c_0; 1) - A(z_0; c_0; 1))$ to the real axis. For $|x| = \epsilon$ small, the main contribution to $\Re(A(x; c_0; 1))$ comes from the term ax^{-1}. So $\Re(A(x; c_0; 1))$ is positive at $x = \epsilon > 0$ and negative at $x = \epsilon < 0$, so the level lines cross the real axis at 0. For $x = 1 - \epsilon$ with ϵ small, the main contribution to $\Re(A)$ comes from the term $\log|1 - x|$. This implies that $\Re(A)$ is negative $x = 1 - \epsilon$, so the level lines cross the real axis somewhere between 0 and 1. For large x, the main contribution to $\Re(A)$ comes from bx, so $\Re(A)$ is positive for large x. Therefore the level lines cross the real axis at a third point. Since $A'(z) = -b(z - z_0)^3 z^{-2}(1 - z)^{-1}$ is positive for $z < z_0$, negative for $z \in (z_0, 0) \cup (0, 1)$, and positive for $z > 1$, the levels lines cannot intersect the real axis at any other point.

For a fixed $x \ll 0$, the main contribution to $\Re(A(x))$ comes from bx, so $\Re(A(x))$ is negative. However, as y increases, $\Re(A(x + iy))$ goes to $+\infty$, since the main contributions come from $c_0 \log|x + iy| + \log|1 - x - iy|$, and $c_0 > -1$. This means there must be level lines going off to infinity. Restricting $\Re(A(z; c_0; 1))$ to a circle $|z| = R \gg 1$ shows that these are the only level lines that go to infinity. Indeed, note that $\Re(A(z; c_0; 1)) > 0$ if $z = R$, and as z moves counterclockwise around the circle, the main contribution to the changes in $\Re(A(z))$ comes from bz. Thus $\Re(A(z))$ decreases as z moves counterclockwise around the circle in the upper half-plane, so the circle can intersect at most one level line in the upper half-plane.

In the upper half-plane, there are four level lines coming from the critical point z_0. We know that three of these lines cross the real axis, while one of them goes off to infinity. Since they can only intersect at z_0, the only possibility is a picture as shown in Fig. 15. This justifies the existence of the contours.

These deformations cause the kernel to pick up residues at $u = w$. The expression for these residues is

$$-\frac{1}{2\pi i} \oint \frac{z^{x_i - x_j - 1}}{(1 - z)^{n_j - n_i}} \, dz \tag{17}$$

where the integral goes around a circle $|z| < 1$. If $n_i \leqslant n_j$, then expression (17) cancels with the z-contour in expression (5). If $n_i > n_j$, then explicitly evaluating the integral yields

$$-(-1)^{x_j - x_i} \binom{n_i - n_j}{x_j - x_i}.$$

The binomial can be approximated by the Demoivre–Laplace Theorem. For large N,

$$-N^{1/4} z_0^{x_j - x_i} (1 - z_0)^{n_j - n_i} (-1)^{x_j - x_i} \binom{n_i - n_j}{x_j - x_i} \approx -\frac{1}{\sqrt{2\pi (t_i - t_j)}} \exp\left(-\frac{(s_j - s_i)^2}{2(t_i - t_j)} \right).$$

So when $t_i > t_j$, we obtain the extra exponential term in Eq. (14).

For large values of N, all the contributions to the double integral come from near the point z_0. Taking the Taylor expansion around z_0 yields

$$N\left(A\left(z; c_0 + \frac{\tilde{t}_m}{N^{1/2}} + \frac{u_m}{N^{3/4}}; 1 + \frac{2t_m}{N^{1/2}} \right) - A\left(z_0; c_0 + \frac{\tilde{t}_m}{N^{1/2}} + \frac{u_m}{N^{3/4}}; 1 + \frac{2t_m}{N^{1/2}} \right) \right) = s_m z' + t_m (z')^2 - (z')^4 + o(1)$$

where $z' = z_0^{-1} \zeta^{-1} N^{1/4} (z - z_0)$. This suggests the substitutions

$$u' = z_0^{-1} \zeta^{-1} N^{1/4} (u - z_0), \qquad w' = z_0^{-1} \zeta^{-1} N^{1/4} (w - z_0).$$

By making these substitutions, we are zooming in at the point z_0 in Fig. 15. Then u' is integrated as shown in Fig. 13 while w' is integrated as shown in Fig. 14.

The exponential terms in expression (16) converge to the exponential terms in (14). The term $\frac{du\, dw}{u-w}$ turns into $z_0 \zeta N^{-1/4} \frac{du'\, dw'}{u'-w'}$. For large N, the contributions to the correlation kernel become focused around z_0, so the extra w in the denominator becomes z_0^{-1}. The proof of Theorem 4.9 is complete. □

Acknowledgments

The authors are very grateful to Grigori Olshanski for a number of valuable suggestions. We would also like to thank the referee for many helpful remarks. The first named author (A.B.) was partially supported by the NSF grant DMS-0707163.

Appendix A. Generalities on random point processes

Let $\mathfrak{X}$ be a locally compact separable topological space. A *point configuration* X in $\mathfrak{X}$ is a locally finite collection of points of the space $\mathfrak{X}$. For our purposes it suffices to assume that the points of X are always pairwise distinct. Denote by $\mathrm{Conf}(\mathfrak{X})$ the set of all point configurations in $\mathfrak{X}$.

A relatively compact Borel subset $A \subset \mathfrak{X}$ is called *a window*. For a window A and $X \in \mathrm{Conf}(\mathfrak{X})$, set $N_A(X) = |A \cap X|$ (number of points of X in the window). Thus, N_A is a function on $\mathrm{Conf}(\mathfrak{X})$. $\mathrm{Conf}(\mathfrak{X})$ is equipped with the Borel structure generated by functions N_A for all windows A.

A *random point process* on $\mathfrak{X}$ is a probability measure on $\mathrm{Conf}(\mathfrak{X})$. One often uses the term *particles* for the elements of a random point configuration.

Given a random point process on $\mathfrak{X}$, one can usually define a sequence $\{\rho_n\}_{n=1}^{\infty}$, where ρ_n is a symmetric measure on $\mathfrak{X}^n$ called the nth *correlation measure*. Under mild conditions on the point process, the correlation measures exist and determine the process uniquely.

The correlation measures are characterized by the following property: For any $n \geqslant 1$ and a compactly supported bounded Borel function f on $\mathfrak{X}^n$ one has

$$\int_{\mathfrak{X}^n} f\rho_n = \left\langle \sum_{x_{i_1},\dots,x_{i_n}\in X} f(x_{i_1},\dots,x_{i_n}) \right\rangle_{X\in\mathrm{Conf}(\mathfrak{X})}$$

where $\langle\cdot\rangle$ denotes averaging with respect to our point process, and the sum on the right is taken over all n-tuples of pairwise distinct points of the random point configuration X.

Often one has a natural measure μ on $\mathfrak{X}$ (called *reference measure*) such that the correlation measures have densities with respect to $\mu^{\otimes n}$, $n = 1, 2, \dots$. Then the density of ρ_n is called the nth *correlation function* and it is usually denoted by the same symbol ρ_n.

The first correlation function ρ_1 is often called the *density function* as it measures the average density of particles.

For point processes on a finite or countable discrete space $\mathfrak{X}$ it is natural to choose the counting measure as the reference measure μ, and then there is a simpler way to define the correlation functions: For any $n = 1, 2, \dots$ and any pairwise distinct $x_1, \dots, x_n \in \mathfrak{X}$,

$$\rho_n(x_1,\dots,x_n) = \mathrm{Prob}\big\{X \in \mathrm{Conf}(\mathfrak{X}) \;\big|\; X \supset \{x_1,\dots,x_n\}\big\}.$$

If $\mathfrak{X}$ is discrete, a random point process on $\mathfrak{X}$ is always uniquely determined by its correlation functions.

The reader can find more information on random point processes in [15].

A point process on $\mathfrak{X}$ is called *determinantal* if there exists a function $K(x, y)$ on $\mathfrak{X}\times\mathfrak{X}$ such that the correlation functions (with respect to some reference measure) are given by the determinantal formula

$$\rho_n(x_1,\dots,x_n) = \det\big[K(x_i,x_j)\big]_{i,j=1}^{n}$$

for all $n = 1, 2, \dots$. The function K is called the *correlation kernel*.

Note that the correlation kernel is not defined uniquely: $K(x, y)$ and $\frac{f(x)}{f(y)}K(x, y)$ define the same correlation functions for an arbitrary nonzero function f on $\mathfrak{X}$.

Assume that $\mathfrak{X}$ is discrete. Define a map Δ by

$$\Delta : \mathrm{Conf}(\mathfrak{X}) \to \mathrm{Conf}(\mathfrak{X}), \quad X \mapsto \mathfrak{X}\backslash X.$$

Given a point process $\mathcal{P}$ on $\mathfrak{X}$, its pushforward under Δ is also a point process on $\mathfrak{X}$; denote it by $\mathcal{P}_\Delta$. The map Δ is often referred to as *particle-hole involution*, because the particles of $\mathcal{P}_\Delta$ are located exactly at those points of $\mathfrak{X}$ where there are no particles of $\mathcal{P}$. With this notation, we have the following proposition.

Proposition A. *If $\mathcal{P}$ is a determinantal point process with correlation kernel $K(x, y)$, then $\mathcal{P}_\Delta$ is also a determinantal point process with correlation kernel*

$$K_\Delta(x, y) = \delta_{x,y} - K(x, y).$$

The proof is an application of the inclusion–exclusion principle, see Proposition A.8 of [8].

Appendix B. Determinantal structure of the correlation functions

Let $\mathfrak{X}_1, \dots, \mathfrak{X}_N$ be finite sets, and

$$\begin{aligned}
&\phi_n(\cdot,\cdot) : \mathfrak{X}_n \times \mathfrak{X}_{n+1} \to \mathbb{C}, \quad n = 1, \dots, N-1,\\
&\phi_n(\mathrm{virt}, \cdot) : \mathfrak{X}_{n+1} \to \mathbb{C}, \quad n = 0, \dots, N-1,\\
&\Psi_j^N(\cdot) : \mathfrak{X}_N \to \mathbb{C}, \quad j = 0, \dots, N-1,
\end{aligned}$$

be arbitrary functions on the corresponding sets. Here the symbol virt stand for a "virtual" variable, which is convenient to introduce for notational purposes. In applications virt can sometimes be replaced by $+\infty$ or $-\infty$.

Set $\mathfrak{X} = \mathfrak{X}_1 \sqcup \mathfrak{X}_2 \sqcup \cdots \sqcup \mathfrak{X}_N$, and to any point configuration $X \in \mathrm{Conf}(\mathfrak{X})$ (the definition of $\mathrm{Conf}(\mathfrak{X})$ can be found in Appendix A) assign its weight $W(X)$ as follows. The weight $W(X)$ is zero unless X has exactly n points in each $\mathfrak{X}_n$, $n = 1, \dots, N$. In the latter case, denote the points of X in $\mathfrak{X}_n$ by x_k^n, $k = 1, \dots, n$. Thus,

$$X = \left\{ x_k^n \;\middle|\; k = 1, \dots, n;\ n = 1, \dots, N \right\}.$$

Set

$$W(X) = \prod_{n=1}^{N-1} \det\left[\phi_n\left(x_i^n, x_j^{n+1}\right)\right]_{i,j=1}^{n+1} \cdot \det\left[\Psi_{N-i}^N\left(x_j^N\right)\right]_{i,j=1}^{N},$$

where $x_{n+1}^n = \mathrm{virt}$ for all $n = 1, \dots, N$.

In what follows we assume that the partition function of our weights does not vanish:

$$Z_N := \sum_{X \in \mathrm{Conf}(\mathfrak{X})} W(X) \neq 0.$$

Under this assumption, the normalized weights $\widetilde{W}(X) = W(X)/Z_N$ define a (generally speaking, complex valued) measure on $\mathrm{Conf}(\mathfrak{X})$ of total mass 1. Using the terminology of Appendix A, one can say that we have a (complex valued) random point process on $\mathfrak{X}$, and its correlation functions are defined accordingly. We are interested in computing these correlation functions.

We need to introduce more notation. Define

$$\phi^{(n_1,n_2)}(x, y) = \begin{cases} (\phi_{n_1} * \cdots * \phi_{n_2-1})(x, y), & n_1 < n_2,\\ 0, & n_1 \geqslant n_2, \end{cases}$$

where we use the notation $(f * g)(x, y) = \sum_z f(x, z) f(z, y)$, and the sum is taken over all possible values of z. For $n = 1, \dots, N$, set

$$\Psi_j^n(x) = \left(\phi^{(n,N)} * \Psi_j^N\right)(x) = \sum_{y \in \mathfrak{X}_N} \phi^{(n,N)}(x, y) \Psi_j^N(y), \quad j = 0, \dots, N-1.$$

Finally, introduce an $N \times N$ matrix M by

$$M_{ij} = \bigl(\phi_{i-1} * \Psi^i_{i-j}\bigr)(\text{virt}) = \sum_{x \in \mathfrak{X}_i} \phi_{i-1}(\text{virt}, x)\Psi^i_{i-j}(x), \quad i, j = 1, \ldots, N.$$

The following statement is a part of Lemma 3.4 in [7].

Proposition B. *The random point process on $\mathfrak{X}$ defined by the weights $\widetilde{W}$ above is determinantal. If we denote the value of the correlation kernel of the process at $x_1 \in \mathfrak{X}_{n_1}$ and $x_2 \in \mathfrak{X}_{n_2}$ by $K(n_1, x_1; n_2, x_2)$, then one choice of the correlation kernel is given by*

$$K(n_1, x_1; n_2, x_2) = -\phi^{(n_1, n_2)} + \sum_{k=1}^{N} \Psi^{n_1}_{n_1-k}(x_1) \sum_{l=1}^{n_2} \bigl[M^{-1}\bigr]_{kl} \bigl(\phi_{l-1} * \phi^{(l, n_2)}\bigr)(\text{virt}, x_2).$$

Remark. One shows that the assumption $Z_N \neq 0$ that we imposed above, is equivalent to the fact that the matrix M is invertible. In fact, up to a sign one has $Z_N = \det M$.

The proof of Proposition B given in [7] is based on the algebraic formalism of [12]. Another proof can be found in Section 4.2 of [17]. A more general statement, where the determinantal property holds for a wider class of measures, was proved as Theorem 4.2 in [6], and a different proof is available in Section 4.4 of [16].

Although we stated Proposition B for the case when all sets $\mathfrak{X}_n$ are finite, one easily extends it to a more general setting. Indeed, the determinantal formula for the correlation functions is an algebraic identity, and the limit transition to the case when $\mathfrak{X}_n$ are allowed to be countably infinite is immediate, under the assumption that all the sums needed to define the $*$-operations above are absolutely convergent. Another easy extension (which we do not need in this paper) is the case when the spaces $\mathfrak{X}_j$ become continuous, and the sums approximate the corresponding integrals over these spaces.

References

[1] A. Aptekarev, P. Bleher, A. Kuijlaars, Large n limit of Gaussian random matrices with external source, part II, Comm. Math. Phys. 259 (2) (2005) 367–389, arXiv:math-ph/0408041v1.

[2] J. Baik, P. Deift, K. Johansson, On the distribution of the length of the longest increasing subsequence of random permutations, J. Amer. Math. Soc. 12 (4) (1999) 1119–1178, arXiv:math/9810105v2.

[3] J. Baik, P. Deift, K. Johansson, On the distribution of the length of the second row of a Young diagram under Plancherel measure, Geom. Funct. Anal. 10 (4) (2000) 702–731, arXiv:math/9901118v1.

[4] P. Biane, Approximate factorization and concentration for characters of symmetric groups, Int. Math. Res. Not. 2001 (4) (2001) 179–192.

[5] A. Borodin, Periodic Schur process and cylindric partitions, Duke Math. J. 140 (3) (2007) 391–468, arXiv:math/0601019v1.

[6] A. Borodin, P. Ferrari, Large time asymptotics of growth models on space-like paths I: PushASEP, arXiv:0707.2813v2.

[7] A. Borodin, P. Ferrari, M. Prähofer, T. Sasamoto, Fluctuation properties of the TASEP with periodic initial configuration, J. Stat. Phys. 129 (2007) 1055–1080, arXiv:math-ph/0608056v3.

[8] A. Borodin, A. Okounkov, G. Olshanski, Asymptotics of Plancherel measures for symmetric groups, J. Amer. Math. Soc. 13 (3) (2000) 481–515, arXiv:math/9905032v2.

[9] A. Borodin, G. Olshanski, Harmonic analysis on the infinite-dimensional unitary group and determinantal point processes, Ann. of Math. (2) 161 (3) (2005) 1319–1422, arXiv:math/0109194v2.

[10] A. Borodin, G. Olshanski, Stochastic dynamics related to Plancherel measure on partitions, Amer. Math. Soc. Transl. Ser. 2 217 (2006) 9–22, arXiv:math-ph/0402064v2.
[11] A. Borodin, G. Olshanski, Asymptotics of Plancherel-type random partitions, J. Algebra 313 (1) (2007) 40–60, arXiv:math/0610240v2.
[12] A. Borodin, E. Rains, Eynard–Mehta theorem, Schur process, and their pfaffian analogs, J. Stat. Phys. 121 (3–4) (Nov. 2005) 291–317.
[13] E. Brezin, S. Hikami, Level spacing of random matrices in an external source, Phys. Rev. E (3) 58 (6) (1998) 7176–7185, part A, arXiv:cond-mat/9804024v1.
[14] E. Brezin, S. Hikami, Universal singularity at the closure of a gap in a random matrix theory, Phys. Rev. E (3) 57 (4) (1998) 4140–4149, arXiv:cond-mat/9804023v1.
[15] D. Daley, D. Vere-Jones, An Introduction to the Theory of Point Processes: Vol. I. Elementary Theory and Methods, Springer-Verlag, New York, 2003.
[16] P. Forrester, E. Nordenstam, The anti-symmetric GUE minor process, arXiv:0804.3293v1.
[17] P. Forrester, T. Nagao, Determinantal correlations for classical projection processes, arXiv:0801.0100v1.
[18] K. Johansson, Discrete orthogonal polynomial ensembles and the Plancherel measure, Ann. of Math. (2) 153 (1) (2001) 259–296, arXiv:math/9906120v3.
[19] K. Johansson, Discrete polynuclear growth and determinantal processes, Comm. Math. Phys. 242 (2003) 277–329, arXiv:math/0206208v2.
[20] S.V. Kerov, Distribution of symmetry types of high rank tensors, Zap. Nauchn. Sem. LOMI 155 (1986) 181–186, (in Russian); English translation in J. Soviet Math. (New York) 41 (2) (1988) 995–999.
[21] S.V. Kerov, Asymptotic Representation Theory of the Symmetric Group and Its Applications in Analysis, Transl. Math. Monogr., vol. 219, Amer. Math. Soc., 2003.
[22] B.F. Logan, L.A. Shepp, A variational problem for random Young tableaux, Adv. Math. 26 (1977) 206–222.
[23] I.G. Macdonald, Symmetric Functions and Hall Polynomials, The Clarendon Press, Oxford University Press, New York, 1995.
[24] A. Okounkov, Random Matrices and Random Permutations, Int. Math. Res. Not. 2000 (20) (2000) 1043–1095, arXiv:math/9903176v3.
[25] A. Okounkov, Symmetric functions and random partitions, in: Symmetric Functions 2001: Surveys of Developments and Perspectives, in: NATO Sci. Ser. II Math. Phys. Chem., vol. 74, Kluwer Acad. Publ., Dordrecht, 2002, pp. 223–252, arXiv:math/0309074v1.
[26] A. Okounkov, G. Olshanski, Asymptotics of Jack polynomials as the number of variables goes to infinity, Int. Math. Res. Not. 1998 (13) (1998) 641–682.
[27] A. Okounkov, N. Reshetikhin, Correlation function of Schur process with application to local geometry of a random 3-dimensional Young diagram, J. Amer. Math. Soc. 16 (3) (2003) 581–603, arXiv:math/0107056v3.
[28] A. Okounkov, N. Reshetikhin, Random skew plane partitions and the Pearcey process, Comm. Math. Phys. 269 (3) (2007) 571–609, arXiv:math/0503508v2.
[29] G. Olshanski, The problem of harmonic analysis on the infinite dimensional unitary group, J. Funct. Anal. 205 (2) (2003) 464–524, arXiv:math/0109193v1.
[30] M. Prähofer, H. Spohn, Scale invariance of the PNG droplet and the Airy process, J. Stat. Phys. 108 (5–6) (2002) 1071–1106, arXiv:math/0105240v3.
[31] C. Tracy, H. Widom, The Pearcey process, Comm. Math. Phys. 263 (2006) 381–400, arXiv:math/0412005v3.
[32] A. Vershik, S. Kerov, Asymptotics of the Plancherel measure of the symmetric group and the limit form of Young tableaux, Soviet Math. Dokl. 18 (1977) 527–531.
[33] A. Vershik, S. Kerov, Characters and factor representations of the infinite unitary group, Soviet Math. Dokl. 26 (1982) 570–574.
[34] A. Vershik, S. Kerov, Asymptotics of the maximal and typical dimension of irreducible representations of symmetric group, Funct. Anal. Appl. 19 (1) (1985) 25–36.
[35] D. Voiculescu, Représentations factorielles de type II_1 de $U(\infty)$, J. Math. Pures Appl. 55 (1976) 1–20.
[36] D.P. Zhelobenko, Compact Lie Groups and Their Representations, Nauka, Moscow, 1970 (in Russian); English translation in Transl. Math. Monogr., vol. 40, Amer. Math. Soc., Providence, RI, 1973.